Marine biodegradation of tailor-made polyhydroxyalkanoates (PHA) influenced by the chemical structure and associated bacterial communities

Gabrielle Derippe, Léna Philip, Pierre Lemechko, Boris Eyheraguibel, Anne-Leïla Meistertzheim, Mireille Pujo-Pay, Pascal Conan, Valérie Barbe, Stéphane Bruzaud, Jean-François Ghiglione

Title: Marine biodegradation of tailor-made polyhydroxyalkanoates (PHA) influenced by the chemical structure and associated bacterial communities

Authors: Gabrielle Derippe[1,2], Léna Philip[1,3], Pierre Lemechko[4], Boris Eyheraguibel[5], Anne-Leïla Meistertzheim[3], Mireille Pujo-Pay[1], Pascal Conan[1], Valérie Barbe[6], Stéphane Bruzaud[2] and Jean-François Ghiglione[1*]

Affiliations :

1. CNRS, Sorbonne Université, UMR 7621, Laboratoire d'Océanographie Microbienne (LOMIC), 1 Avenue Fabre, F-66650 Banyuls sur mer, France
2. Université Bretagne Sud, Institut de Recherche Dupuy de Lôme (IRDL), UMR CNRS 6027, 56321 Lorient, France
3. SAS Plastic@Sea, Observatoire Océanologique de Banyuls, France
4. Institut Régional des Matériaux Avancés (IRMA), 2 all. Copernic, 56270 Ploemeur, France
5. Université Clermont Auvergne, Clermont Auvergne INP, CNRS, Institut de Chimie (ICCF), Clermont– Ferrand, France.
6. Génomique Métabolique, Genoscope, Institut François Jacob, CEA, CNRS, Univ Evry, Université Paris-Saclay, Evry, France

(*) Corresponding author: Jean-François Ghiglione, Laboratoire d'Océanographie Microbienne (LOMIC), 1 Avenue Fabre, F-66650 Banyuls sur mer, Email : ghiglione@obs-banyuls.fr

Keywords: Polyhydroxyalkanoate (PHA), Biosynthesis, Biodegradation, Plastisphere

Abstract

Over recent years, biodegradable polymers have been proposed to reduce environmental impacts of plastics for specific applications. The production of polyhydroxyalkanoates (PHA) by using diverse carbon sources provides further benefits for the sustainable development of biodegradable plastics. Here, we present the first study evaluating the impact of physical, chemical and biological factors driving the biodegradability of various tailor-made PHAs in the marine environment. Our

multidisciplinary approach demonstrated that the chemical structure of the polymer (i.e. the side chain size for *short-* vs. *medium-chain* PHA) which was intrinsically correlated to the physico-chemical properties, together with the specificity of the biofilm growing on plastic films (i.e. the associated 'plastisphere') were the main drivers of the PHA biodegradation in the marine environment.

Environmental implication:

Plastic pollution of the environment is a critical problem that has the potential for long-lasting impact. While all plastics eventually break down to at least some degree, they can remain in different transition states for extended periods of time, such as microplastics and nanoplastics, that represent different types of hazards. PHA currently occupy a growing portion of the biodegradable plastics market and relevant studies on their biodegradation are needed to address potential environmental problems.

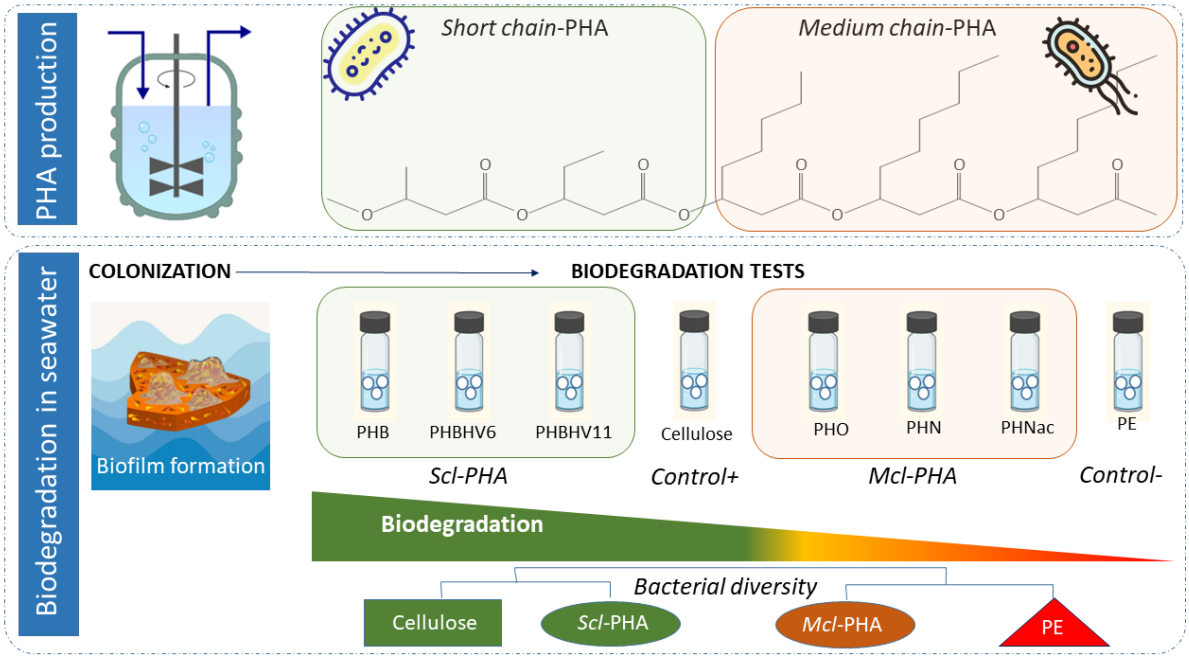

1.Introduction

Plastic pollution is nowadays a global and evident environmental crisis that is of major concern to marine organisms (Deudero and Alomar, 2015), but also contributes to raise global greenhouse gas emissions and climate change (Shen et al., 2020). The marine environment constitutes a large reservoir of mismanaged plastic waste, with 4.8 to 12.7 million metric tons of plastic entering

the oceans every year (Jambeck et al., 2015). As a partial solution, it has been proposed to manufacture plastics that would be both bio-based, i.e. made from renewable resources, and biodegradable in a given environment (compost, soil, water) over a reasonable amount of time (weeks, months). The biodegradable plastics have been considered relevant for selected applications with respect to their use and end of life (Paul-Pont et al., 2023). Among the bio-based and biodegradable polymers, polyhydroxyalkanoates (PHA) are considered as a promising alternative to fossil-based or non-biodegradable polymers. Mainly but not only from bacterial origin, the PHA constitute a large family and display a wide range of chemical compositions and properties according to the producing strain, the source of carbon used for feeding and the fermentation process. PHA can be divided into two subgroups: short chain-length PHA (*scl*-PHA) composed of monomers of 3 to 5 carbon atoms, and medium chain-length PHA (*mcl*-PHA) composed of monomers of 6 to 14 carbon atoms. The physico-chemical properties differ between the *scl*-PHA, that are rigid and brittle polymers and the *mcl*-PHA that are usually more rubbery and ductile (Pérez-Rivero and Hernandez-Raquet, 2017). Poly(3-hydroxybutyrate) (PHB) is one of the most widespread and best characterized among the PHA. With high crystallinity (>50%), it is a relatively brittle and stiff polymer (Corre et al., 2012; Koller et al., 2010). Production of the copolymer with valeric acid triggers the incorporation of 3-hydroxyvalerate (HV) and results in the less stiff and brittle copolymer poly(3-hydroxybutyrate-co-3-hydroxyvalerate) (PHBHV), easier to process for commercial applications (Lemechko et al., 2019; Pachekoski et al., 2009). *Mcl*-PHA display properties that could replace elastomers. They are rubbery, soft and show a lower degree of crystallinity, melting temperature and glass transition (Abe et al., 2012). Despite the recent interest in their properties for biomedical or cosmetic applications, *mcl*-PHA are not produced in industrial quantities and the relationships between their biodegradation and their physico-chemical properties have been poorly explored (Abe et al., 2012).

Biofilm growing on plastic is characterized by very diverse and niche-specific microbial communities called the “plastisphere” (Zettler et al., 2013) that can play a predominant role in plastic degradation (Jacquin et al., 2019). Previous studies showed the great abilities of microbial communities to biodegrade *scl*-PHA in the marine environment (Deroiné et al., 2014; Volant et al., 2022). The microbial communities colonizing commercial PHBHV under marine conditions have been

studied during semi- and long-term colonization, but no clear relation was made with the rate of biodegradation (Dussud et al., 2018; Odobel et al., 2021). Due to the limited commercial availabilities, no studies have ever reported microbial activity and diversity on *mcl*-PHA, thus resulting in a lack of comparison between the environmental end of life of plastics made of *scl*- or *mcl*-PHA families.

In this study, we describe the bacterial production of 6 different tailor-made *scl*- and *mcl*-PHA by *Halomonas sp. SF200*3 (Thomas et al., 2019) and *Pseudomonas putida KT2440 (DSM 6125),* respectively, together with their physico-chemical characterization. We also analysed their biodegradation by using a two steps protocol including a one-month pre-colonisation step in a flow-through aquarium with natural seawater for each PHA group (*scl*- and *mcl*-PHA) and controls (cellulose and Polyethylene, PE) to mimic the growth of marine natural biofilms and another step in minimum medium with plastics as sole carbon source to test biodegradation. We hypothesized that various PHA types, related chemical and physical properties, as well as the associated natural biofilms, are driving the biodegradation in seawater. We used a multidisciplinary approach to produce (bioreactor) and characterize six tailor-made PHA (gas chromatography, steric exclusion chromatography, contact angles, differential scanning calorimetry) and to evaluate the bacterial diversity (16S rDNA Illumina sequencing) associated to the biodegradation (oxygen consumption, heterotrophic bacterial production) of each polymer type.

2.Materials and methods

2.1. Production of *scl*- and *mcl*-PHAs

Pre-cultures of *Halomonas sp.* SF2003 for *scl*-PHA production and *Pseudomonas putida* KT2440 for *mcl*-PHA production were both performed in 500 mL Erlenmeyer flasks at 30 °C and 200 rpm, with incubations for 8 h in Zobell media (Thomas et al., 2019) or for 16 h in mineral medium (Maclean et al., 2008), respectively. The preculture was then transferred into a 5 L bioreactor (GPC-BIO, MINIPROLAB, France) containing a final volume of 2 L of Zobell medium or mineral medium for *scl*- and *mcl*-PHA production, respectively. Cultivation temperature was 30 °C, pH 7.0 ± 0.2. Agitation was at a minimum of 400 rpm to maintain a dissolved oxygen concentration above 30 %, as measured with optical dissolved oxygen sensors (Hamilton company, Switzerland).

Prior to PHA accumulation from different carbon sources, *scl*-PHA fermentation started with 10 $g.L^{-1}$ of glucose to promote growth. After 12 h, one pulse of 5 $g.L^{-1}$ of glucose was added every 4 hours until 24 h for the PHB accumulation. A mix of glucose and valeric acid (50/50, %mol) was continuously dropped in the bioreactor at a rate of 4 $mL.h^{-1}$ for 24 h for the poly-(3-hydroxybutyrate-co-3-hydroxyvalerate) (PHBHV6) fermentation. A mix of glucose and valeric acid (70/30, % mol) was continuously dropped at a rate of 6 $mL.h^{-1}$ for 24 h for the PHBHV11 fermentation. *Mcl*-PHA fermentation also started with glucose implementation to promote high cell density before PHA accumulation, as previously described (Sun et al., 2006). Briefly, this included a first phase of 24 h growth with a feeding strategy based on pulses of exponential quantity of glucose over 7 h (12.5 $g.L^{-1}$ of glucose) followed by a linear feeding strategy from 7 to 24 h by adding a pulse of 1 g of glucose additionally to the previous quantity of glucose pulsed every hour. After 24 h, 1 g of fatty acids (octanoic, heptanoic or nonanoic acid or a mix of nonanoic acid and acrylic acid) was added to produce a poly(3-hydroxyoctanoate) (PHO), a poly(3-hydroxynonanoate) (PHN) and another PHN called “PHNac”, respectively) was added when the dissolved oxygen concentration was above 30% (approximately every 15 minutes).

At the end of the fermentation, bacterial cells were recovered by centrifugation and PHA were separated from bacterial biomass using an incubation with an excess of solvent under stirring in a glass bottle (50 mL of chloroform for approximately 1 g of *scl*-PHA at 60°C overnight and 40 mL of dichloromethane at room temperature overnight for approximately 1 g of *mcl*-PHA). For *scl*-PHA extraction, distilled water (V/V) was added after cooling. The suspension was mixed and centrifuged to recover the organic layer before filtration on glass fiber cotton and casting in a glass Petri dish. *Mcl*-PHA solution were filtered through a 1.2 µm glass microfiber and the concentrated *mcl*-PHA solution was precipitated in cold ethanol (10% v/v) and stored at 6 °C for two days before collection. The casting process consisted of dissolving PHA in their respective solvents, pouring PHA solutions into a glass Petri dish covered with lids that were opened briefly twice a day until constant weight to allow slow solvent evaporation. Films were stored at room temperature and in the dark during three weeks before any characterizations. Thickness of the films ranged from 80 to 120 µm for all PHA films.

2.2. Physico-chemical characterization of the six tailor-made PHA films

Compositions of the produced PHA were determined by gas chromatography (GC). *Scl*-PHA and *mcl*-PHA underwent a propanolysis (Riis and Mai, 1988) and a methanolysis (Furrer et al., 2007), respectively. Briefly, 10 mg of PHA were dissolved in 1 mL of chloroform or dichloromethane and further propyl esterified (*scl*-PHA) with 1 mL of a solution of 1-propanol/37% HCl (8/2, V/V) or methyl esterified (*mcl*-PHA) with 1 mL of MeOH/BF3 (10% Boron trifluoride, V/V) at 80°C for 20 h. After cooling down, distilled water (V/V) was added and the solutions were vortexed. The organic phase was retrieved, dried on $MgSO_4$, filtered on glass fiber cotton and samples were injected on a Perkin Elmer Clarus 480 gas chromatograph equipped with a 30 m x 0.32 mm DB–5 column (HP) with splitless injector and flame ionization detector (FID). Oven temperature, ramp and nitrogen flow were measured according to Riis and Mai (1988) and Furrer et al. (2007).

Molecular weights were measured by steric exclusion chromatography (SEC) using an Agilent Technologies 1200 Infinity II containing an isocratic pump, a column oven at 35 °C and a RI detector. PHA sample separations were performed by two columns PLgel (Mixed-E, 3 µm and Mixed-D, 5 µm) from Polymer Laboratories for *scl*-PHA and by two columns from Malvern Panalytical technologies (LT4000L, 4µm and LT5000L, 10 µm) for *mcl*-PHA and a column guard. About 10 mg of PHA were first dissolved into 2 mL of chloroform (*scl*-PHA) or THF (*mcl*-PHA) then filtered with PTFE filter (0,45 µm) before a 50 µL injection. The calibration was done with polystyrene standards from Agilent Technologies.

Contact angles were measured on each PHA films using a drop shape analyser from KRÜSS scientific technologies with a 2 µL droplet of water placed on the top surface-air side of the solvent-cast films that have been previously stabilized for 3 weeks at room temperature. More than 5 measurements were carried out for a single sample and the resulting values were averaged.

Thermal properties were determined by differential scanning calorimetry (DSC) using a Mettler-Toledo DSC-882 equipment. About 6 mg of PHA were taken from the cast films of PHA. Particular attention was given so that all the PHA samples experienced the same thermal history (3 weeks ageing at room temperature in the dark for all solvent-casted films) in order to avoid the

induction of different structures, as reported elsewhere (Crétois et al., 2016; Laycock et al., 2014; Xie et al., 2008). PHA samples were equilibrated to 25°C then heated to 190 °C for *scl*-PHA or 80°C for *mcl*-PHA at 10 °C.min^{-1} and kept isothermal for 2 min followed by a cooling down to -40 °C for *scl*-PHA or -70 °C for *mcl*-PHA at 10 °C.min^{-1}. A second isotherm at -40 °C or -70 °C was kept for 2 min then the sample was heated from -40 to 190 °C or -70 °C to 80 °C at 10 °C.min^{-1} according to the PHA type. Melting temperatures and melting enthalpies were measured from the first heating ramp for while glass transition temperatures were measured on the second heating ramp and values correspond to the inflection point (Appendice A).

2.3. Experimental setup of the biodegradation assay

A two phase stepwise experiment (Appendix B) was designed in order to evaluate the biodegradability of the polymers under marine conditions, as previously described (Cheng et al., 2022). Briefly, the first step consisted of the formation of a mature biofilm on each PHA groups : PHBHV (from Tianan biological materials, China, 40 µm thickness) was used for the colonization of the *scl*-PHA group including PHB, PHBHV6 and PHBHV11; PHO (produced as described above, 120 µm thickness) was used for the colonization for *mcl*-PHA including PHO, PHN and PHNac) together with a positive control (Cellulose filter colonization, CELLU, Whatman 42, thickness 200 µm) and a negative control (Blow Low Density polyethylene colonization, PE, Symphony Environmental Technology, UK, thickness 50µm). Large rectangular pieces of 13.5 cm^2 of each polymer type mentioned above were incubated for one month (5 August to 6 September 2021) in separate 2.4 L aquarium with continuous circulating seawater (flow rate ranged from 8 to 12 mL.min^{-1}) pumped in the Banyuls bay (NW Mediterranean Sea). Throughout the experiment, seawater temperature (between 19 °C and 24 °C) and salinity (38.5 g.L^{-1}) in the aquarium were similar to seawater from the Banyuls bay. Secondly, individual biofilms were detached from two pieces of each PHA or PE or Cellulose colonized films by three cycles of 1 min vortex and 3 min sonication and resuspended in a 40 mL of carbon-minimum medium called “MM” hereafter (Appendix C). Cell numbers were verified by flow cytometry (FACSCanto II flow cytometer, BD Bioscience, San Jose, CA) and adjusted to the exact same concentration 10^5 cells.mL^{-1} by dilution of each detached biofilm in MM, in order to ensure

comparable inoculum concentration between biodegradation tests. Previous tests using different detached biofilm concentration (from 10^4 to 10^6 cells.mL^{-1}) showed that it was an optimal concentration under our experimental conditions, according to the carrying capacity of the biofilm on plastics (data not shown) and also in accordance to the classical bacterial concentration found in seawater (Pulido-Villena et al., 2012). Three sterile discs of 6 mm^2 diameter each of each PHA solvent-casted films (PHB, PHBHV6, PHBHV11, PHO, PHN and PHNac, total surface of 60 ± 0.5 mm^2), PE (total surface of 59 mm^2) and Cellulose (total surface of 64 mm^2) were then placed in sterile 12 mL Exetainer tubes (Exetainer flat bottom 12 mL, Labco, Lampeter, UK) together with 3 mL of the corresponding inoculum previously detached. The tubes were incubated in the dark at 18 ± 0.25°C under agitation at 110 rpm (orbital agitator, Innova® S44i, Eppendorf, Germany) for a 2-month period (called "biotic conditions" hereafter). In addition, similar incubation and sampling procedure were used for abiotic controls, which consisted of triplicate vials containing 3 mL of MM with plastics of the same composition (called "abiotic condition" hereafter). A total of 887 tubes were needed to follow the different parameters detailed below, with triplicates samples taken after 0, 1, 15, 30 and 60 days of incubation.

2.4. Continuous oxygen measurement

During the second step of the experiment, duplicate vials with each plastic type were equipped with an optical fiber luminescent oxygen sensor (SP-PSt5, Presens, Germany) and oxygen concentration was monitored using a small 24-channel reader (SDR SensorDish®, Presens, Germany). Oxygen sensors were placed in the liquid phase to obtain the concentration of dissolved oxygen recorded every hour over 60 days. In the case of *scl*-PHA and cellulose, vials were opened under a sterile laminar flow hood after 30 days to ensure that oxygen was not limiting for bacterial growth and closed again. In this case, oxygen concentration was always maintained at > 50 µmol L^{-1} (20% absolute oxygen), and the re-opening for 10 minutes was enough to return to initial values (around 235 µmol L−1), as previsouly described (Cheng et al., 2022).Oxygen consumption was expressed in µmol(O_2).mm^2. Total surface of the three discs were taken into account: 3*(top and bottom: $\pi*r^2$ and exposed edges: 2*π*r*h).

2.5. Heterotrophic Bacterial Production

Heterotrophic Bacterial Production (BP) was measured on triplicate samples for each PHA type at 15, 30 and 60 days by ^{3}H-leucine incorporation into proteins, as previously described (Dussud et al., 2018). Briefly, a soft cell detachment pre-treatment based on three cycle of vortex and sonication was first performed. Then, ^{3}H-leucine (specific activity of 112 Ci.$mmol^{-1}$) was added onto PHA samples (final concentration of 1 nmol.L^{-1} after addition of cold leucine). Radioactivity was measured using a Beckman Scintillation Counter (LS 5000CE) after addition of trichloroacetic acid (TCA) 50% and resuspension in a liquid scintillation cocktail (Ultima Gold). An empirical conversion factor of 1.55 ng C.$pmol^{-1}$ of incorporated leucine was used to calculate BP (Simon and Azam, 1989). Blanks followed the same protocol but bacterial activity was stopped by the introduction of 50% TCA prior to the addition of the radioactive mix. BP was expressed in ng(C).mm^2.h^{-1}. Total surface of one disc was taken into account: (top and bottom: $\pi*r^2$ and exposed edges: 2*π*r*h).

2.6. DNA extraction and sequencing.

Plastic pieces were sampled at 15, 30 and 60 days and stored at -80°C until DNA extraction. One litre seawater was sampled from the control aquarium, then successively filtered through 3-µm

and 0.2-µm pore size polycarbonate filters (PC, 47 mm diameter, Nucleopore), and filters were stored at -80°C. We also sampled the initial biofilm previously detached after the first one-month colonisation step on PHBHV, PHO, cellulose and PE films, which was stored at -80°C after filtration onto 0.2-µm pore size polycarbonate filters (PC, 47 mm diameter, Nucleopore). DNA extractions were realized on all samples using the same phenol-chloroform method, as previously described (Odobel et al., 2021). Primers used for PCR amplification of the 16S V3–V5 region were 515F-Y and 926R (Fuhrman et al., 1989), previously shown as well-suited for marine samples (Parada et al., 2016). Sequencing was performed on Illumina MiSeq by Genoscope (Evry, France), generating 3,060,721 paired sequences in the 29 samples. Raw FASTA files were deposited at EBI under the accession number ERP148254. Sequence analysis was processed using the package DADA2 (Version 1.24.0) into R studio software (R Core Team, 2022, version 4.2.2). A standard pipeline was applied with the following parameters: trimLeft= c(19,20), truncLen= c(240,240), maxN=0, maxEE=c(2,2), truncQ=2. The sequences were therefore filtered, dereplicated, denoised by removing sample interference and chimeras before merging. Clusters were assigned with the Silva 128 16S rRNA database (Quast et al., 2013) and clusters that did not belong to Bacteria kingdom were removed as well as chloroplast and mitochondrial sequences. The number of sequences per sample was normalized by rarefaction (n= 21,324) and a table with 29 samples and 5,053 amplicon sequence variants (ASV) was obtained.

2.7. Statistical analysis

All graphical representations and statistical analysis were performed on R studio software (R Core Team, 2022, version 4.2.2) using the packages ggplot2 (Wickham, 2016), vegan (Oksanen et al., 2007) and phyloseq (McMurdie and Holmes, 2012) and PRIMER6 (Clarke and Gorley, 2006). Data were compared with Kruskal-Wallis tests followed by post hoc tests at D60 for oxygen consumption and heterotrophic bacterial production. Sequences were analyzed with the phyloseq package. The alpha diversity indexes were calculated and compared with Wilcoxon tests. Differences in microbial community structure among samples were tested by ANOSIM based on Bray-Curtis distances (PRIMER6 software). The ASVs that contributed most to differentiate microbial community structures between *scl*-PHA *vs*. PE, *scl*-PHA *vs*. *mcl*-PHA and *mcl*-PHA *vs*. PE were tested with a similarity percentage analysis (SIMPER, PRIMER6) (Clarke, 1993).

3.Results

3.1. Physico-chemical characterization of the six tailor-made PHA

Three fermentation processes in a bioreactor with *Halomonas sp. SF2003* growing on different substrates resulted in the production of three *scl*-PHA: PHB, PHBHV6 and PHBHV11 (Table 1). *Halomonas sp. SF2003* growing on glucose accumulated a homopolymer of PHB composed at 100% of 3-hydroxybutyrate units (HB) (Table 1) with 4.00 carbons per monomer. A mix of glucose and valeric acid (70/30, % mol) resulted in PHBHV11 production composed of 89% of HB and 11% of HV, leading to an average number of 4.11 carbons per monomer. PHBHV6 was produced using another mix of glucose and valeric acid (50/50, % mol) resulting in a copolymer composed of 94% of HB and 6% of HV with an average number of 4.06 carbons per monomer. Fermentations from *Pseudomonas putida KT2440* from two different fatty acids (octanoic and nonanoic acid) and a β-oxidation pathway inhibitor (acrylic acid) (Jiang et al., 2013) led to three *mcl*-PHA: PHO, mainly composed of 3-hydroxyoctanoate (HO) monomer (89%), then 3-hydroxyhexanoate (HHx) and 3-hydroxydecanoate (HD) (5.5% each) for an average number of 7.78 carbons per monomer, PHN was composed of 3-hydroxynonanoate (HN) monomer units (58%) plus HD (24%), 3-hydroxyheptanoate (HHp) (14%) and HO (4%) units with an average number of 8.92 carbons per monomer and PHNac composed of HN (73%), HHp (23%) and HD (2%) with an average number of 8.47 carbons per monomer.

Thermal properties of all PHA were characterized by DSC (Table 1, Appendix A). *Scl*-PHA displayed glass transition temperatures between -7°C and 4°C. *Scl*-PHA with HV units (PHBHV6 and PHBHV11) showed slightly lower peaks of melting temperatures (171 for PHBVHV6 and 172 °C for PHBHV11) compared to PHB (177 °C). Melting enthalpies also differed according to the chemical composition. Higher melting enthalpy is observed for PHB (ΔH_m = 89 $J.g^{-1}$) then followed by PHBHV6 (ΔH_m = 60 $J.g^{-1}$) and finally by PHBHV11 (ΔH_m = 30 $J.g^{-1}$) due to the presence of HV units which partially limit the chain crystallisation. Number average molecular mass could not be measured for PHB due to solubility difficulties. PHBHV6 and PHBHV11 displayed $\overline{M_n}$ of 340 000 and 325 000 $g.mol^{-1}$ with a dispersity index (Đ) of 2.8 and 2.9, respectively. Among *scl*-PHA, contact angles with

distilled water revealed that PHB is the least hydrophobic polymer with a contact angle of 64 ± 1.6 °, followed by PHBHV11 (74 ± 1 °) and PHBHV6 (76 ± 2 °). On the other hand, *mcl*-PHA displayed lower glass transition temperatures (PHO: -36 °C, PHN: -40 °C and PHNac: -39 °C) and lower melting temperatures (PHO: 57 °C, PHN: 49 °C and PHNac: 52 °C) than all *scl*-PHA. Melting enthalpies is also far lower than *scl*-PHA with a melting enthalpy of 20 $J.g^{-1}$ for PHO and PHN and a lower one of 13 $J.g^{-1}$ for PHNac. $\overline{M}_n$ of *mcl*-PHA ranged from 60 000 to 84 000 $g.mol^{-1}$ with a Đ ranging from 2.2 to 2.7. High hydrophobicity is displayed by *mcl*-PHA, especially for PHN (90 ± 2 °) then for PHO and PHNac (82 ± 2 ° and 80 ± 1 °, respectively). Overall, physico-chemical properties of the PHA produced differed greatly according to the type of PHA (*scl*- or *mcl*-) while slight but noticeable differences were found within both PHA types.

Table 1: Composition of the 6 tailor-made PHA and their associated thermal characteristics, average molecular mass and contact angle.

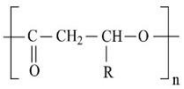	**Chemical composition**	**Average number of carbon per monomer**	**$\overline{M}_n$ (g. mol^{-1})**	**Đ**	**T_g (°C)**	**T_m (°C)**	**ΔH_m ($J.g^{-1}$)**	**Contact angle (°)**
PHB	100% HB	$C_{4.00}$	-	-	4	177	89	64 ± 2
PHBHV6	94% HB 6% HV	$C_{4.06}$	340 000	2.8	-7	171	60	76 ± 2
PHBHV11	89% HB 11% HV	$C_{4.11}$	325 000	2.9	-7	172	30	74 ± 1
PHO	5.5% HX 89% HO 5.5% HD	$C_{7.78}$	84 000	2.2	-36	57	20	82 ± 2
PHN	14% HHp 4% HO 58.1% HN 24% HD	$C_{8.92}$	60 000	2.7	-40	49	20	90 ± 2
PHNac	23% HHp 74% HN 2%HD	$C_{8.47}$	70 000	2.2	-39	52	13	80 ± 1

3.2. Biodegradation activities

Several parameters were used to evaluate the biodegradability of the various PHA. Firstly, abiotic controls (PHA, CELLU or PE) did not show signs of contamination and chemical oxygen demand was negligible in our conditions.

Secondly, continuous oxygen consumption (Presens sensors) by microorganisms with PHA as sole carbon and energy source showed a clear distinction between *scl*- and *mcl*-PHA. During the first 15 days, oxygen consumption rapidly increased and tended to reach a plateau from 15 to 60 days for the *mcl*-PHA while it kept increasing to a greater extent for *scl*-PHA (Fig. 1A). At day 60, PHB (mean = 4.47 ± 0.23 x 10^{-3} µmol(O_2).mm^{-2}), PHBHV6 (mean = 4.37 ± 0.57 x 10^{-3} µmol(O_2).mm^{-2}), and PHBHV11 (3.39 ± 0.23 10^{-3} µmol(O_2).mm^{-2}) presented a much higher oxygen consumption than PHO (0.18 ± 0.02 x 10^{-3} µmol(O_2).mm^{-2}), PHN (0.70 ± 0.11 x 10^{-3} µmol(O_2).mm^{-2}), and PHNac (0.31 ± 0.02 x 10^{-3} µmol(O_2).mm^{-2}). Significant difference was found between *scl*- and *mcl*-PHA biodegradation ($p<0.05$), as well as with between *scl*- and the PE control (0,72 ± 0.09 x 10^{-4} µmol(O_2).mm^{-2}, $p<0.05$). No significant difference was found between the oxygen consumption on *scl*-PHA compared to Cellulose (2.08 ± 0.12 x 10^{-3} µmol(O_2).mm^{-2}, $p > 0.05$). Likewise, a kinetic comparison between within *scl*-PHA or within *mcl*-PHA did not show any statistical differences. Among *mcl*-PHA, small but noticeable oxygen consumption was observed for PHN, while PHO and PHNac had a similar trend to the PE negative control.

Thirdly, cell incorporation of ^{3}H-leucine into proteins showed similar trends, with significantly higher heterotrophic activities for *scl*-PHA as compared to *mcl*-PHA. Within the first 15 days of incubation in minimum medium, the activities of the biofilms were high and then decreased until day 60 for all the PHA (Fig. 1B). At day 60, maximum activities were found for the positive control cellulose (2.35 ± 1.08 x 10^{-1} ng(C).mm^{-2}.h^{-1}) and *scl*-PHA, including PHBHV6 (2.67 ± 0.97 x 10^{-1} ng(C).mm^{-2}.h^{-1}), PHB (2.58 ± 0.31 x 10^{-1} ng(C).mm^{-2}.h^{-1}) and PHBHV11 (2.28 ± 0.85 x 10^{-1} ng(C).mm^{-2}.h^{-1}). Much lower bacterial activities were observed for the negative control PE (0.95 ± 0.58 x 10^{-2} ng(C).mm^{-2}.h^{-1}) and *mcl*-PHA, including PHN (0.77 ± 0.30 x 10^{-1} ng(C).mm^{-2}.h^{-1}), PHNac (0.49 ± 0.20 x 10^{-1} ng(C).mm^{-2}.h^{-1}), PHO (0.21 ± 0.10 x 10^{-1} ng(C).mm^{-2}.h^{-1}), that significantly differed from cellulose ($p<$ 0.05).

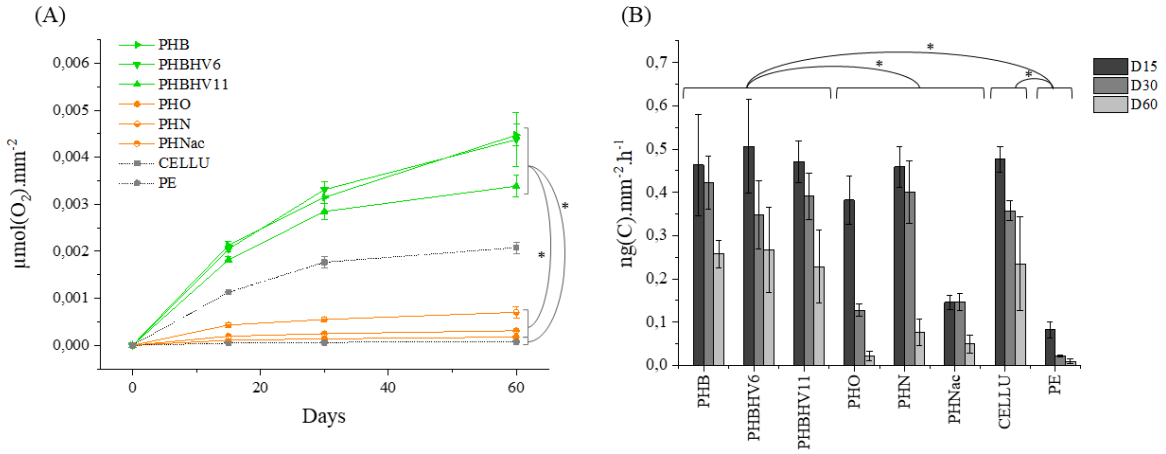

Figure 1: Cumulative oxygen consumption (A) and bacterial heterotrophic production (B) on the different polymers (green: PHB, PHBHV6, PHBHV11; orange: PHO, PHN and PHNac and grey: CELLU and PE) in minimum media for 15, 30, 60 and 90 days. Errors bars indicate standard deviation. * indicates significant difference by Kruskal-Wallis test on day 60 (n = 24).

3.3. Bacterial diversity

During the 60-days of experiment, no significant change in alpha-diversity was observed in all polymer types over time, including all the measured diversity indexes (Chao1 richness, Pielou evenness, Shannon and Simpson diversity) ($p > 0.05$) (Table 2). However, significant differences were found between the polymer groups, including cellulose and *scl*-PHA (PHB, PHBHV6 and PHBHV11), as compared to another group including PE and *mcl*-PHA (PHO, PHN and PHNac) ($p < 0.05$). Lower Chao1 richness and Shannon diversity were found for *scl*-PHA (244.4 ± 8.8 and 3.3 ± 0.3; n = 9, respectively) as compared to *mcl*-PHA (606.8 ± 19.4 and 4.4 ± 0.4; n = 9, respectively) ($p = 1.6 \times 10^{-4}$). Higher diversity on the free-living bacteria and on the initial inocula for each polymer type was also observed (Table 2).

Table 2: Total number of ASV per sample together with *Chao*1 richness, Pielou eveness and Shannon, and Simpson diversity indexes. SW: seawater, INOC: microbial inoculum from each polymer types after one month of colonization, D: incubation time in days.

Sample	Total ASV	*Chao*1	Pielou	Shannon	Simpson
SW-FREE	939	1313	0.716	4.9	57.8
SW-ATT	497	541	0.644	4	18.3
INOC_CELLU	707	889	0.671	4.4	25.5
CELLU_D60	207	226	0.656	3.5	15.5
CELLU_D30	288	322	0.636	3.6	12.7
CELLU_D15	128	129.	0.556	2.7	5.8
INOC_SCL	651	656.	0.818	5.3	75.4
INOC_MCL	1276	1425	0.755	5.4	42.9
PHBHV11_D15	307	331	0.559	3.2	8.2
PHBHV11_D30	166	171	0.548	2.8	6.3
PHB_D15	313	343	0.574	3.3	11.4
PHB_D30	243	264	0.564	3.1	11.4
PHB_D60	213	246	0.653	3.5	18
PHBHV11_D60	266	294	0.591	3.3	10.9
PHBHV6_D30	212	237	0.672	3.6	14.8
PHBHV6_D60	156	163	0.733	3.7	27
PHBHV6_D15	147	148	0.561	2.8	8
PHN_D60	423	528	0.678	4.1	23.5
PHNac_D15	435	470	0.691	4.2	23.8
PHNac_D30	517	560	0.640	4	14.5
PHNac_D60	403	472	0.650	3.9	20.7
PHN_D15	434	498	0.692	4.2	25.4
PHN_D30	290	302	0.776	4.4	45.3
PHO_D15	689	767	0.719	4.7	48.7
PHO_D30	753	879.	0.740	4.9	58.4
PHO_D60	822	983	0.775	5.2	74.7
PE_D60	711	828	0.701	4.6	31.3
PE_D30	616	676	0.747	4.8	65.5
PE_D15	547	614	0.793	5	82.7

Beta-diversity analysis showed four distinct groups between bacterial communities living on cellulose, *scl*-PHA (PHB, PHBHV6 and PHBHV11), *mcl*-PHA (PHO, PHN and PHNac), PE and in seawater (Fig. 2). Interestingly, inoculum grown on cellulose before the experiment grouped with the bacterial communities living on cellulose as sole carbon source. In contrast, this was not the case for *scl*-PHA and *mcl*-PHA inocula, that changed when incubated with the different polymer types. ANOSIM analysis showed significant differences between *scl*-PHA and *mcl*-PHA samples (R = 0.964,

p < 0.05). Within these groups, no clear distinction could be made between samples, except for PHBHV6 (day 15 and 60) for *scl*-PHA and PHO-D60 for *mcl*-PHA.

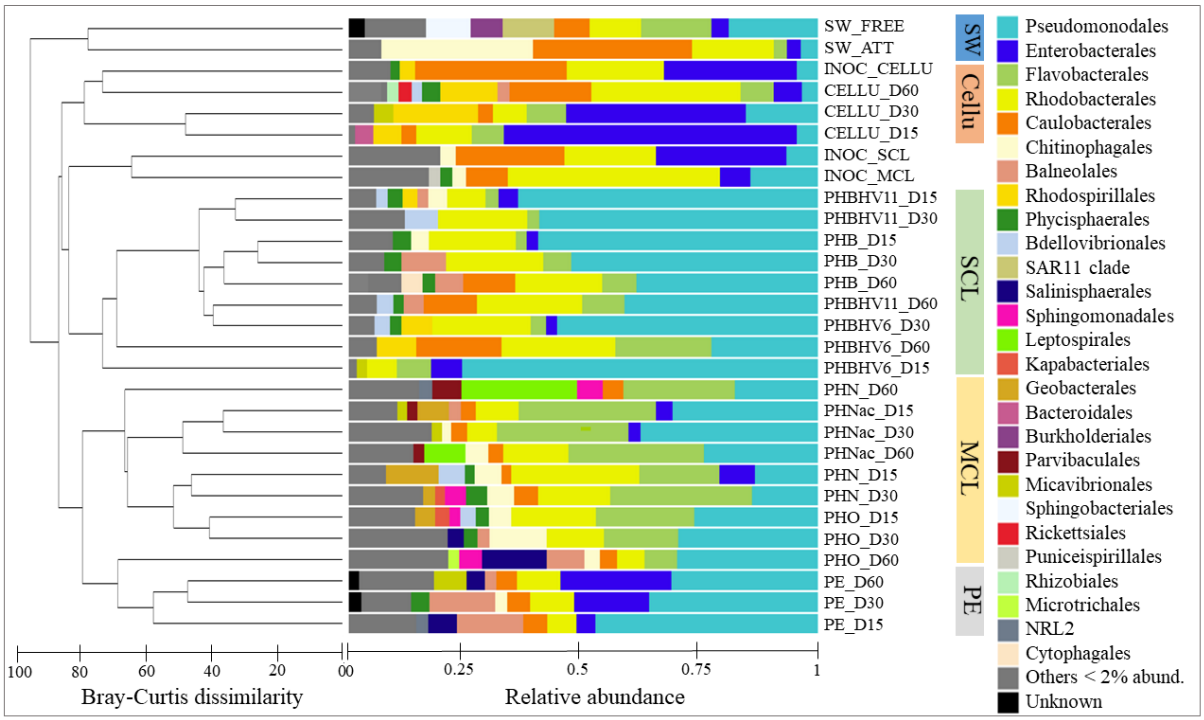

Figure 2: Comparison of community structures and taxonomic abundances of bacteria in seawater (SW), on the microbial inoculum from each polymer types after one month of colonization (INOC) and bacteria on polymers (PHB, PHBHV6, PHBHV11, PHO, PHN and PHNac) according to time (in days, D), by UPGMA dendrogram based on Bray-Curtis dissimilarities between sequencing profiles (left) and by cumulative bar charts comparing relative order abundances (right).

Taxonomic composition confirmed the niche-partitioning between the bacterial communities living in seawater compared to the plastisphere of the different polymer types. Free-living bacteria were composed of Pseudomonodales (19%), Flavobacteriales (15%), Rhodobacterales (11%), SAR11 clade (11%), Sphingobacteriales (9%) and Caulobacterales (8%), while organic particle-attached bacteria were dominated by Caulobacterales (34%), Chitinophagales (32%) and Rhodobacterales (17%). The inoculum pre-grown on cellulose in seawater was mainly composed of Caulobacterales (32% for INOC_CELLU), Rhodobacterales (21% for INOC_CELLU), Enterobacterales (28% for INOC_CELLU) and to a lesser extent of Pseudomonodales (5% for INOC_CELLU). The same groups were also found for the inocula pre-grown on *scl*-PHA and *mcl*-PHA but with different proportions,

including Caulobacterales (23% for INOC_SCL and 9% for INOC_MCL), Rhodobacterales (20% for INOC_SCL and 45% for INOC_MCL), Enterobacterales (28% for INOC_SCL and 7% for INOC_MCL) and Pseudomonodales (5% for INOC_CELLU, 7% for INOC_SCL and 14% for INOC_MCL). After inoculation with the different polymer types as sole carbon source, the proportion of different taxa was different between the different polymer types. Pseudomonodales were high on *scl*-PHA (52 ± 15 %, n=9), *mcl*-PHA (25 ± 2%, n=9), PE samples (28 ± 7%, n=3) and cellulose (8 ± 5%, n=3) together with Rhodobacterales (mean = 18 ± 6%, 13 ± 7%, 8 ± 1%, 17 ± 10%, n=9 for *scl*-PHA, *mcl*-PHA, PE and cellulose, respectively). *Mcl*-PHA exhibited high proportions of Flavobacteriales (mean = 22 ± 7%, n = 9) compared to other polymers (between 0% on PE and 10% on others polymer). The main taxa found on cellulose was Enterobacterales (mean = 35 ± 23%, n = 3), especially on CELLU_J15 and CELLU_J30 (Fig. 2).

SIMPER analysis on the Bray Curtis dissimilarity index highlighted two species contributing to the differences between *scl*-PHA and PE. First, ASV affiliated to *Marinobacter sp.* showed a high relative abundance in *scl*-PHA (more than 37%) and a high contribution (20%) (Fig. 3) compared to PE. *Cobetia sp*. is the second most specific species found on *scl*-PHA in a lesser abundance (10%) and contributes to 6% on *scl*-PHA. Those two species that display a clear distinction between *scl*-PHA and PE microbial communities also contributed to the differences found between *scl*-PHA and *mcl*-PHA. Indeed, *Marinobacter sp.* and *Cobetia sp.* were poorly represented on *mcl*-PHA, while a major relative abundance and contribution were found for *Pseudomonas sp.* (12% and 7% for relative abundance and contribution, respectively) and Flavobacteriaceae (11% and 6% for relative abundance and contribution, respectively) for this polymer type. Additionally, *Pseudomonas sp.* and Flavobacteriaceae were poorly represented on *scl*-PHA, as well as on PE. Bacterial communities observed on *mcl*-PHA and PE seemed richer and more scattered. With the exception of Rhodobacterales that were abundant on all polymer types, taxa belonging to *Alcanivorax sp.* (13% and 8% of relative abundance and contribution, respectively), Balneolaceae, Pseudomonodales, Alloalcanivorax, Alcanivoraceae and Alteromonodaceae found on PE were poorly abundant on *scl*-PHA. Taxa belonging to Alloalcanivorax and Alcanivoraceae were also present on *mcl*-PHA but presented low contribution (2%) when compared to PE.

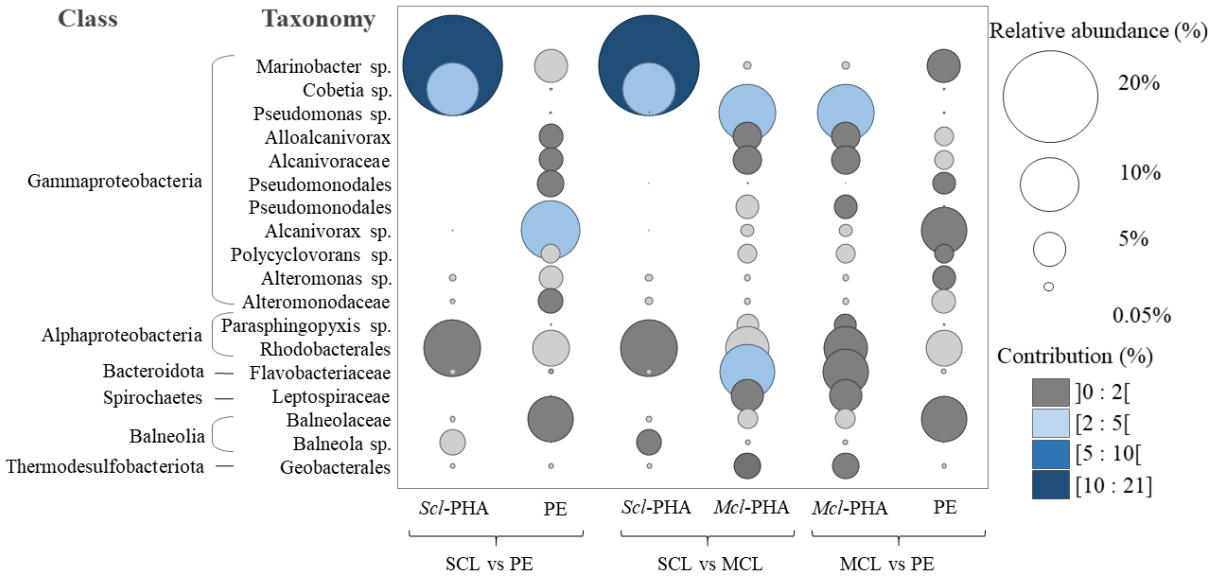

Figure 3: Bubble plot showing the relative abundance and the taxonomy of the majority ASV contributing to 50% of the dissimilarity between *scl*-PHA *vs. mcl*-PHA, *scl*-PHA *vs*. PE and *mcl*-PHA *vs.* PE. Points are sized according to the relative abundance and colored by their contribution to dissimilarity.

4. Discussion

4.1. Different physico-chemical characteristics of the six tailor-made PHA

The first step of this study was to produce three *scl*-PHA and three *mcl*-PHA with various intrinsic properties in order to estimate the influence of the physico-chemical characteristics in the PHA biodegradation in the marine environment. The bacterial strain *Halomonas sp.* SF2003 has been used for the production of *scl*-PHA using glucose and/or valeric acid to generate PHB, PHBV6 and PHBV11. Surprisingly, an increase of valeric acid in the substrate feeding led to a lower HV content in PHBHV6. Valeric acid was added to the medium in the form of a mix of valeric acid and glucose. Since it was continuously dropped at a slow rate (4 mL.min^{-1}), it led to the permanent presence of low valeric acid concentration in the bioreactor but also glucose concentration. *Halomonas sp. SF2003 cells* seem, in this particular conditions (on two permanently available substrates), metabolize glucose for HB accumulation at the expense of valeric acid and therefore HV incorporation in the polymer. The use of different substrates induced different chemical compositions that affect thermal properties. HV incorporation tended to slightly lower the glass transition temperatures changed from -7 to 4 °C

with 11 and 6% of HV proportions. Melting temperatures dropped from 177 °C to 172 °C and 171 °C with 11% and 6% of HV incorporation, respectively. Overall, DSC analysis showed common features found in other *scl*-PHA produced and characterized in the literature (Koller et al., 2010; Lemechko et al., 2019; Możejko-Ciesielska and Kiewisz, 2016). The melting enthalpy, comparable to the PHA crystallinity, was a parameter influenced by the HV incorporation due to a higher steric hindrance generated by the HV units compared to that of HB units. It tended to decrease as much as the HV content increased to reach 30 $J.g^{-1}$ with 11% of HV unit. The modulation of HV unit proportion, even at low incorporation, is a promising way to modify the PHA properties, for instance to bring softness and elasticity to the homopolymer PHB, which can show some difficult features to process due to its high crystallinity and a melting temperature close to its degradation temperature (Pachekoski et al., 2013). Regarding *mcl*-PHA, different chain lengths and/or monomer proportions have been achieved, thus impacting to a certain extent the intrinsic properties of each of these *mc*l-PHA. PHO was mainly composed of HO (89%), PHN was mainly composed of HN (58%) and the addition of acrylic acid improved the HN content in PHNac (74%). Improving the HN content in PHNac seemed to mainly modify the crystallinity, since the melting enthalpy drops from 20 to 13 $J.g^{-1}$ in this latter polymer. Generally, thermal properties between *mcl*-PHA slightly differ and are in accordance with PHA composed of these monomers (Abe et al., 2012; Możejko-Ciesielska and Kiewisz, 2016). Tailor-made production with different strains and carbon sources allowed to produce PHA displaying clear and significant distinctions between *scl*- and *mcl*-PHA, including thermal properties, molecular weights or hydrophobicity.

4.2. Various biodegradation activities on the different polymer types

The main originality of our study is to present pioneer results of microbial biodegradation activities of the various tailor-made PHA under natural marine conditions. Particular attention has been made here to produce PHA samples through the same process and of the same shape and size. Special care was also taken to mimic the polymer biodegradation capabilities of natural mature biofilm growing on plastics, by using pre-colonized biofilms on each *scl*- and *mcl*-PHA as test inoculum (or biofilm growing on PE and cellulose for controls), as previously described (Cheng et al., 2022).

Previous studies underlined the lack of environmental representability of standard test methodologies, which was due in particular to the inadequate test inoculum (Harrison et al., 2018; Napper and Thompson, 2020; Paul-Pont et al., 2023). In particular, the use of seawater as test inoculum is not representative of the biofilm growing on plastic, since the two communities were shown to clearly differ in term of biodiversity and functions (Bryant et al., 2016; Zettler et al., 2013). Moreover, mature biofilm formed on conventional plastic (such as PE) were shown to be different from biodegradable plastics (such as PHA or cellulose) (Odobel et al. 2021). This is the reason why the first step consisted of the formation of a mature biofilm on each PHA groups (*scl*- and *mcl*-PHA), as well as on PE and cellulose controls. In addition, a minimum medium with no carbon source was used to avoid false positive signals, together with the addition of nutrient according to Redfield N:P ratio classically used in marine biodegradation tests (16:1) (Van Wambeke et al., 2009). Most of the evidence for PHA biodegradability in marine environment focused previously on weight loss (Deroiné et al., 2015, 2014; López-Ibáñez and Beiras, 2022; Volova et al., 2011). Weight loss provides a proof of the plastic disintegration only, which may or may not be associated to the complete mineralization by bacteria (Haider et al., 2019). There is a consensus in using the last mineralization step as a relevant proof of plastic biodegradability, either estimated by O_2 uptake or CO_2 release (Jacquin et al. 2019). Here, we measured the O_2 uptake directly on the aqueous phase by using the 'plastic-free' Presens® optical dissolved oxygen sensors, which have been proven to give similar response and with less abiotic losses compared to other commercially available manometric test systems, such as the Oxitop® device (Brown et al. 2018). It was particularly well suited for the large number of replicate samples tested in this study, and allowed the use of 12mL Exetainer tubes with perfect sealing that fitted in only one incubator for better reproducibility and with strict thermal regulation (± 0.25°C) that reduced variation in O_2 values. With PHA being the sole carbon source in our biodegradation tests, the trend of oxygen consumption and microbial activities on *scl*-PHA clearly demonstrated their biodegradability in seawater, thus confirming previous observations by using other techniques (Deroiné et al., 2015, 2014; Volant et al., 2022).

Under laboratory conditions and by using pure bacterial culture, PHA biodegradation processes were depicted to be the result of specialized extracellular enzymes called PHA

depolymerases (Leathers et al., 2000; Mukai et al., 1993). The enzymes are capable of hydrolysing PHA chains into smaller water-soluble compounds (< 600 Da) that can cross the membranes for further bacterial degradation and assimilation (Azam and Malfatti, 2007). In our study, respiration associated to the *scl*-PHA assimilation by bacteria resulted in a regular increase in oxygen consumption during the 60 days of biodegradation tests. The respiration rates were higher than with the cellulose positive control in the same experimental conditions, whereas it was almost undetectable on PE negative control. Bacterial heterotrophic activity (^{3}H-Leucine incorporation) on *scl*-PHA as sole carbon source showed the same trend, with significantly higher activity on *scl*-PHA than for mcl-PHA and PE. Both oxygen consumption and bacterial heterotrophic activities were high during the first 15 days of tests (even for PE films to a lesser extent), likely due to the organic matter that was detached together with the pre-colonized biofilm or due to mortality, thus rendering this period of the biodegradation tests less adequate for biodegradation measurement under our conditions. A similar difference in bacterial heterotrophic production between PHBHV and PE films was previously found during long-term colonization and biodegradation (Dussud et al., 2018; Odobel et al., 2021). Within the *scl*-PHA group, we observed slight but significantly higher oxygen consumption on PHB and PHBHV6 compared to PHBHV11 after 60 days. Such a difference was not found for bacterial heterotrophic activities, rendering the difference in biodegradation within the *scl*-PHA less robust. Contrasting results found in the literature confirmed the possible but not consistent difference in biodegradation rates for these two polymers. A hypothesis of better biodegradation abilities of the PHBHV copolymer was linked to an increase of amorphous regions which are more susceptible to enzymatic attack compared to the homopolymer PHB (Meereboer et al., 2020; Numata et al., 2008). Other studies of *in vitro* enzymatic degradation showed the opposite, with better degradation capacities on PHB compared to PHBHV (Mukai et al., 1993). Slight differences in terms of biodegradation between *scl*-PHA are therefore difficult to explain since biodegradation is a combination of physical, chemical and biological factors (Dilkes-Hoffman et al., 2019). As a consequence, we conclude that the intrinsic differences within the *scl*-PHA properties (hydrophobicity, crystallinity, molecular weight) were not sufficient to induce a difference in biodegradation activities in our marine experimental conditions.

In the opposite, signs of biodegradation were very low or almost undetectable for the tested *mcl*-PHA types. By comparison to scl-PHA, very few studies tested the biodegradability of *mcl*-PHA in marine ecosystems, probably because no *mcl*-PHA are commercially available (Lott et al., 2021; Suzuki et al., 2021). The tailor-made *mcl*-PHA produced in this study showed clear distinct chemical differences between PHO, PHN and PHNac. Although PHN showed a slightly higher oxygen consumption and bacterial heterotrophic activities after 60 days than PHO and PHNac, no statistical difference was shown. It is to be noted that oxygen consumption and bacterial heterotrophic activities of the *mcl*-PHA group were similar to the negative control PE, which was a sign of very low or no biodegradability in our marine experimental conditions. We are aware that the 2-month timing of tests was probably not sufficient and we propose to perform further studies with a longer test period before giving a firm conclusion of the absence of biodegradability (in a reasonable period of time) for the *mcl*-PHA.

Interestingly, our study offers a large set of analysis to compare the physico-chemical characteristics of *scl*- and *mcl*-PHA and assess their impact on PHA biodegradation. Although polymers with low number average molecular weight, low crystallinity and low hydrophobicity are expected to show better sign of biodegradation (Kumar et al., 2020), it does not seem to fully explain the difference found in *scl*- and *mcl*-PHA biodegradability with natural inoculum. Indeed, *scl*-PHA produced in this studies were more crystalline with higher number average molecular weight than the *mcl*-PHA but they still showed far greater biodegradation abilities. Then, the differences in physico-chemical characteristics between *scl*- and *mcl*-PHA might not be sufficient to explain the difference observed on biodegradation. As mentioned in previous studies of PHA biodegradation in seawater (Deroiné et al., 2015), no significant changes were observed in molecular weight at the end of the experiment, thus confirming a enzymatic process of degradation that resulted in surface erosion rather than bulk erosion (Appendix D). We hypothesize that biodegradation might also result from the specificity of the extracellular PHA depolymerase to the *scl*- or to the *mcl*-PHA. Indeed, it has been previously shown that the catalytic domain activity differed between *scl*- and *mcl*-PHA depolymerase, rendering the *mcl*-PHA depolymerase ineffective on *scl*-PHA, and inversely (Kim et al., 2000). Moreover, the carbon chain length of *mcl*-PHA (which present a higher molecular mobility compared

to those of *scl*-PHA) could inhibit enzymatic degradation by impeding the catalytic domain with longer side chain length and steric hindrance interferences (Numata et al., 2009). Finally, *mcl*-PHA depolymerases are less abundant than *scl*-PHA depolymerases in several type of environments including the marine environment (Viljakainen and Hug, 2021). These results suggest that the type of PHA mainly influences the biodegradation rate.

4.3. Dissimilar microbial community associated to the various polymer types

Biodegradation is a complex process involving intrinsic (relative to the polymer) but also extrinsic factors (relative to the environment). In this study, we decided to keep the same temperature, mixing, light and nutrients constant to focus on the impact of bacterial diversity as a key factor in plastic biodegradation. First, we paid specific attention to performing the biodegradation tests with realistic biofilm living in the natural marine environment. While there is no consensus today for the preparation of the microbial inocula in the ISO or ASTM standards for polymer biodegradability tests, convergent views indicated that complex natural marine inoculum made of biofilm growing on the corresponding plastics under naturals conditions are recommended (Cheng et al., 2022). A colonisation phase for a minimum of one month in natural seawater has been shown to be a pre-requisite to mimic a mature biofilm in seawater (Jacquin et al., 2019; Odobel et al., 2021), as has been done in this study. Bray-Curtis similarity showed that the biofilms growing during one month in natural seawater were similar in *scl*-PHA and *mcl*-PHA, but different from cellulose or PE films. As previously described in other studies, free-living and particle-attached bacteria living in the seawater presented very different communities compared to the plastisphere of the mature biofilms (Dussud et al., 2018; Wright et al., 2020), thus rendering the use of seawater as inoculum for biodegradation tests irrelevant. We emphasize the value of using inoculum made of pre-formed mature biofilm as an important methodological step forward for biodegradation tests, as previously described (Cheng et al., 2022; Jacquin et al., 2019).

The transfer of pre-formed biofilm from natural seawater to minimum medium resulted in bacterial community changes for *scl*-PHA and *mcl*-PHA, but not for cellulose that remained stable

during the entire 60-day incubation. Following the evolution of the bacterial community changes during the biodegradation tests has been recommended by previous studies (Jacquin et al., 2019; Kowalczyk et al., 2015), but this recommendation has been poorly followed thereafter. Changes in bacterial diversity may be used as a signal of the lack of representability of the biodegradation tests to mimic the natural environment. By following the bacterial diversity for all the tested plastics, we showed that the alpha-diversity remained stable during the course of the second step of the experiment for all plastic types, which is a prerequisite for the biodegradability tests in natural conditions (Jacquin et al., 2019).

The study of the bacterial communities also permitted to describe the potential of some ASVs to be involved in the biodegradation of the *scl*-PHA. SIMPER analysis on Bray-Curtis 16S rRNA dissimilarities showed the importance of *Marinobacter* sp. *and Cobetia sp*. in explaining the difference between the *scl*-PHA and the negative control PE. *Marinobacter* sp. has been previously shown to present abilities to degrade PHB and PHBHV (Kasuya et al., 2000; Martínez-Tobón et al., 2018). These authors demonstrated PHB and PHBHV depolymerase activities of isolated *Marinobacter* strains, and identified the *scl*-PHA depolymerase PhaZ gene. *Cobetia* sp. has never been observed as PHA-degraders, but it is a well-known producer of PHA (Christensen et al., 2021; Moriya et al., 2020). Further studies are needed to evaluate its potential to perform both the production and the degradation of *scl*-PHA using exoenzymes, as it has been shown for other species (Martínez-Tobón et al., 2018; Nygaard et al., 2021). These two strains were much less abundant in PE but also in *mcl*-PHA, thus suggesting a selection in *scl*-PHA associated to its biodegradation under marine conditions. Some specific species were detected in *mcl*-PHA that presented low abundance in PE. This is particularly the case for *Pseudomonas* sp., which were previously shown as very effective producers of *mcl*-PHA (Prieto et al., 2016), with the ability to also produce extracellular *mcl*-PHA depolymerase (Schirmer et al., 1993; Schirmer and Jendrossek, 1994; Young et al., 2005). *Pseudomonas* sp. was also very low in abundance in *scl*-PHA, confirming the selection of different species depending on the *scl*-PHA vs. *mcl*-PHA groups. Further long-term studies will be needed to evaluate if the *Pseudomonas* sp. selected on *mcl*-PHA may be involved in their biodegradation. This first study on *mcl*-PHA opens

new routes for further studies to better understand the bacterial diversity involved in their biodegradation in the marine environment.

Conclusion

PHA are generally cited as one solution among others to replace conventional plastics, that would be both bio-based and biodegradable. Most of the studies so far have proven the rapid biodegradability of *scl*-PHA that are already commercially available, but very few of them investigated the fate of *mcl*-PHA in the environment. To our knowledge, this is the first study comparing the biodegradation of *scl*- and *mcl*-PHA in the marine environment. One strength of our work was to produce six tailor-made PHA with different physico-chemical characteristics, in order to estimate their biodegradation and identify their associated bacterial community. The physico-chemical properties of the PHA studied might not be sufficiently different to have an impact of these characteristics on biodegradation signals within a PHA type. However, this study showed that the chemical nature of the polymer (*short*- vs. *medium-chain* length PHA) together with the diversity of microorganisms living on the plastic films (and probably the associated enzymes, i.e. PHA depolymerase) were the main drivers of the PHA biodegradability in the marine environment. These results are of importance for further application of PHA with different rates of biodegradation for commercial purpose, such as the production of fishing nets, buoys or cosmetic products that potentially end their life in the marine environment (Paul-Pont et al., 2023). This study also showed that *mcl*-PHA biodegradation takes longer than *scl*-PHA, which could suggest the use of this PHA group for longer-lifetime products. Further biodegradation tests with longer period of time (more than 2 months) are needed to better explore the biodegradation of the more recalcitrant *mcl*-PHA, and we believe that this study opens new routes for a better understanding of *scl*-PHA and *mcl*-PHA biodegradation in the marine environment.

Acknowledgements

This project was supported by the PEPS-CNRS "Development of New Biodegradable Biopolymers" in the project "Biodegradability of biosourced polymers such as PolyHydroxyAlkanoates (PHA) in the marine environment (acronym: PHABIO), coordinated by S. Bruzaud & J.F. Ghiglione. It is also part of the EU-funded AtlantECO project (Atlantic Ecosystems Assessment, Forecasting & Sustainability, Horizon 2020 No 862923). We thank David Leistenschneider and Maxime Beauvais for their help launching the whole experiment and we are grateful to Guigui PA, VF, JS, JP for insightful comments on the manuscript. This work was part of the Ph.D thesis of G. Deripp supported by a financial support from the CNRS through the MITI interdisciplinary programs *(*AAP 80|PRIME-2020) and of the Ph.D thesis of L. Philip supported by Plastic@Sea company and the CIFRE program.

Conflict of interest:

The authors declare that they have no known competing financial interests or personal relationships that could have appeared to influence the work reported in this paper.

Author Contributions (CRediT taxonomy)

Gabrielle Deripp: Conceptualization, Formal analysis, Investigation, Methodology, Visualization, Writing - Original Draft, review & editing, **Léna Philip**: Conceptualization, Formal analysis, Investigation, Methodology, Visualization, Writing - review & editing, **Pierre Lemechko:** Formal analysis, Investigation, Writing - review & editing, **Boris Eyheraguibel**: Visualization, Writing - review & editing, **Anne-Leïla Meistertzheim**: Methodology, Visualization, Writing - review & editing, , **Pascal Conan**: Methodology, Visualization, Writing - review & editing, **Mireille Pujo-Pay**: Methodology, Visualization, Writing - review & editing, **Valérie Barbe**: Supervision, Formal analysis, Visualization, Writing - review & editing, **Stéphane Bruzaud:** Conceptualization, Funding acquisition, Methodology, Project administration, Resources, Supervision, Visualization, Writing - review & editing, **Jean-François Ghiglione:** Conceptualization, Funding acquisition, Methodology, Project administration, Resources, Supervision, Visualization, Writing - review & editing.

References

Abe, H., Ishii, N., Sato, S., Tsuge, T., 2012. Thermal properties and crystallization behaviors of medium-chain-length poly(3-hydroxyalkanoate)s. Polymer 53, 3026–3034. https://doi.org/10.1016/j.polymer.2012.04.043

Azam, F., Malfatti, F., 2007. Microbial structuring of marine ecosystems. Nat Rev Microbiol 5, 782–791. https://doi.org/10.1038/nrmicro1747

Bryant, J.A., Clemente, T.M., Viviani, D.A., Fong, A.A., Thomas, K.A., Kemp, P., Karl, D.M., White, A.E., DeLong, E.F., 2016. Diversity and Activity of Communities Inhabiting Plastic Debris in the North Pacific Gyre. mSystems 1, 10.1128/msystems.00024-16. https://doi.org/10.1128/msystems.00024-16

Cheng, J., Eyheraguibel, B., Jacquin, J., Pujo-Pay, M., Conan, P., Barbe, V., Hoypierres, J., Deligey, G., Halle, A.T., Bruzaud, S., Ghiglione, J.-F., Meistertzheim, A.-L., 2022. Biodegradability under marine conditions of bio-based and petroleum-based polymers as substitutes of conventional microparticles. Polymer Degradation and Stability 206, 110159. https://doi.org/10.1016/j.polymdegradstab.2022.110159

Christensen, M., Jablonski, P., Altermark, B., Irgum, K., Hansen, H., 2021. High natural PHA production from acetate in Cobetia sp. MC34 and Cobetia marina DSM 4741T and in silico analyses of the genus specific PhaC2 polymerase variant. Microbial Cell Factories 20, 225. https://doi.org/10.1186/s12934-021-01713-0

Clarke, K., Gorley, R., 2006. "PRIMER v6." User Manual/Tutorial, Plymouth Routine in Multivariate Ecological Research – ScienceOpen.

Clarke, K.R., 1993. Non-parametric multivariate analyses of changes in community structure. Australian Journal of Ecology 18, 117–143. https://doi.org/10.1111/j.1442-9993.1993.tb00438.x

Corre, Y.-M., Bruzaud, S., Audic, J.-L., Grohens, Y., 2012. Morphology and functional properties of commercial polyhydroxyalkanoates: A comprehensive and comparative study. Polymer Testing 31, 226–235. https://doi.org/10.1016/j.polymertesting.2011.11.002

Crétois, R., Chenal, J.-M., Sheibat-Othman, N., Monnier, A., Martin, C., Astruz, O., Kurusu, R., Demarquette, N.R., 2016. Physical explanations about the improvement of PolyHydroxyButyrate ductility: Hidden effect of plasticizer on physical ageing. Polymer, Polymers at Interfaces: Probing Mechanics and Interactions by Atomic Force Microscopy 102, 176–182. https://doi.org/10.1016/j.polymer.2016.09.017

Deroiné, M., César, G., Le Duigou, A., Davies, P., Bruzaud, S., 2015. Natural Degradation and Biodegradation of Poly(3-Hydroxybutyrate-co-3-Hydroxyvalerate) in Liquid and Solid Marine Environments. J Polym Environ 23, 493–505. https://doi.org/10.1007/s10924-015-0736-5

Deroiné, M., Le Duigou, A., Corre, Y.-M., Le Gac, P.-Y., Davies, P., César, G., Bruzaud, S., 2014. Seawater accelerated ageing of poly(3-hydroxybutyrate-co-3-hydroxyvalerate). Polymer Degradation and Stability 105, 237–247. https://doi.org/10.1016/j.polymdegradstab.2014.04.026

Deudero, S., Alomar, C., 2015. Mediterranean marine biodiversity under threat: Reviewing influence of marine litter on species. Marine Pollution Bulletin 98, 58–68. https://doi.org/10.1016/j.marpolbul.2015.07.012

Dilkes-Hoffman, L.S., Lant, P.A., Laycock, B., Pratt, S., 2019. The rate of biodegradation of PHA bioplastics in the marine environment: A meta-study. Marine Pollution Bulletin 142, 15–24. https://doi.org/10.1016/j.marpolbul.2019.03.020

Dussud, C., Hudec, C., George, M., Fabre, P., Higgs, P., Bruzaud, S., Delort, A.-M., Eyheraguibel, B., Meistertzheim, A.-L., Jacquin, J., Cheng, J., Callac, N., Odobel, C., Rabouille, S., Ghiglione, J.-F., 2018. Colonization of Non-biodegradable and Biodegradable Plastics by Marine Microorganisms. Frontiers in Microbiology 9, 1571. https://doi.org/10.3389/fmicb.2018.01571

Fuhrman, J.A., Sleeter, T.D., Carlson, C.A., Proctor, L.M., 1989. Dominance of bacterial biomass in the Sargasso Sea and its ecological implications. Marine Ecology Progress Series 57, 207–217.

Furrer, P., Hany, R., Rentsch, D., Grubelnik, A., Ruth, K., Panke, S., Zinn, M., 2007. Quantitative analysis of bacterial medium-chain-length poly([R]-3-hydroxyalkanoates) by gas chromatography. Journal of Chromatography A 1143, 199–206. https://doi.org/10.1016/j.chroma.2007.01.002

Haider, T.P., Völker, C., Kramm, J., Landfester, K., Wurm, F.R., 2019. Plastics of the Future? The Impact of Biodegradable Polymers on the Environment and on Society. Angewandte Chemie International Edition 58, 50–62. https://doi.org/10.1002/anie.201805766

Harrison, J.P., Boardman, C., O'Callaghan, K., Delort, A.-M., Song, J., 2018. Biodegradability standards for carrier bags and plastic films in aquatic environments: a critical review. R. Soc. open sci. 5, 171792. https://doi.org/10.1098/rsos.171792

Jacquin, J., Cheng, J., Odobel, C., Pandin, C., Conan, P., Pujo-Pay, M., Barbe, V., Meistertzheim, A.-L., Ghiglione, J.-F., 2019. Microbial Ecotoxicology of Marine Plastic Debris: A Review on Colonization and Biodegradation by the "Plastisphere." Front. Microbiol. 10. https://doi.org/10.3389/fmicb.2019.00865

Jambeck, J.R., Geyer, R., Wilcox, C., Siegler, T.R., Perryman, M., Andrady, A., Narayan, R., Law, K.L., 2015. Plastic waste inputs from land into the ocean. Science 347, 768–771. https://doi.org/10.1126/science.1260352

Jiang, X., Sun, Z., Ramsay, J.A., Ramsay, B.A., 2013. Fed-batch production of MCL-PHA with elevated 3-hydroxynonanoate content. AMB Express 3, 50. https://doi.org/10.1186/2191-0855-3-50

Kasuya, K., Mitomo, H., Nakahara, M., Akiba, A., Kudo, T., Doi, Y., 2000. Identification of a Marine Benthic P(3HB)-Degrading Bacterium Isolate and Characterization of Its P(3HB) Depolymerase. Biomacromolecules 1, 194–201. https://doi.org/10.1021/bm9900186

Kim, H.M., Ryu, K.E., Bae, K., Rhee, Y.H., 2000. Purification and characterization of extracellular medium-chain-length polyhydroxyalkanoate depolymerase from Pseudomonas sp. RY-1. J. Biosci. Bioeng. 89, 196–198. https://doi.org/10.1016/s1389-1723(00)88737-x

Koller, M., Salerno, A., Dias, M.M. de S., Reiterer, A., Braunegg, G., 2010. Modern Biotechnological Polymer Synthesis: A Review. Food technology and biotechnology 48, 255–269.

Kowalczyk, A., Martin, T.J., Price, O.R., Snape, J.R., van Egmond, R.A., Finnegan, C.J., Schäfer, H., Davenport, R.J., Bending, G.D., 2015. Refinement of biodegradation tests methodologies and the proposed utility of new microbial ecology techniques. Ecotoxicology and Environmental Safety 111, 9–22. https://doi.org/10.1016/j.ecoenv.2014.09.021

Kumar, G., Anjana, Hinduja, Sujitha, Dharani, 2020. Review on plastic wastes in marine environment – Biodegradation and biotechnological solutions. Marine Pollution Bulletin 150, 110733. https://doi.org/10.1016/j.marpolbul.2019.110733

Laycock, B., Halley, P., Pratt, S., Werker, A., Lant, P., 2014. The chemomechanical properties of microbial polyhydroxyalkanoates. Progress in Polymer Science, Topical Issue on Biorelated Polymers 39, 397–442. https://doi.org/10.1016/j.progpolymsci.2013.06.008

Leathers, T.D., Govind, N.S., Greene, R.V., 2000. Biodegradation of Poly(3-hydroxybutyrate-co-3-hydroxyvalerate) by a Tropical Marine Bacterium, Pseudoalteromonas sp. NRRL B-30083. Journal of Polymers and the Environment 8, 119–124. https://doi.org/10.1023/A:1014873731961

Lemechko, P., Le Fellic, M., Bruzaud, S., 2019. Production of poly(3-hydroxybutyrate-co-3-hydroxyvalerate) using agro-industrial effluents with tunable proportion of 3-hydroxyvalerate monomer units. International Journal of Biological Macromolecules 128, 429–434. https://doi.org/10.1016/j.ijbiomac.2019.01.170

López-Ibáñez, S., Beiras, R., 2022. Is a compostable plastic biodegradable in the sea? A rapid standard protocol to test mineralization in marine conditions. Science of The Total Environment 831, 154860. https://doi.org/10.1016/j.scitotenv.2022.154860

Lott, C., Eich, A., Makarow, D., Unger, B., van Eekert, M., Schuman, E., Reinach, M.S., Lasut, M.T., Weber, M., 2021. Half-Life of Biodegradable Plastics in the Marine Environment Depends on Material, Habitat, and Climate Zone. Frontiers in Marine Science 8.

Maclean, H., Sun, Z., Ramsay, J., Ramsay, B., 2008. Decaying exponential feeding of nonanoic acid for the production of medium-chain-length poly(3-hydroxyalkanoates) by *Pseudomonas putida* KT2440. Can. J. Chem. 86, 564–569. https://doi.org/10.1139/v08-062

Martínez-Tobón, D.I., Gul, M., Elias, A.L., Sauvageau, D., 2018. Polyhydroxybutyrate (PHB) biodegradation using bacterial strains with demonstrated and predicted PHB depolymerase activity. Appl Microbiol Biotechnol 102, 8049–8067. https://doi.org/10.1007/s00253-018-9153-8

McMurdie, P.J., Holmes, S., 2012. Phyloseq: a bioconductor package for handling and analysis of high-throughput phylogenetic sequence data. Pac Symp Biocomput 235–246.

Meereboer, K.W., Misra, M., Mohanty, A.K., 2020. Review of recent advances in the biodegradability of polyhydroxyalkanoate (PHA) bioplastics and their composites. Green Chemistry 22, 5519–5558. https://doi.org/10.1039/D0GC01647K

Moriya, H., Takita, Y., Matsumoto, A., Yamahata, Y., Nishimukai, M., Miyazaki, M., Shimoi, H., Kawai, S.-J., Yamada, M., 2020. Cobetia sp. Bacteria, Which Are Capable of Utilizing Alginate or Waste Laminaria sp. for Poly(3-Hydroxybutyrate) Synthesis, Isolated From a Marine Environment. Frontiers in Bioengineering and Biotechnology 8. https://doi.org/10.3389/fbioe.2020.00974

Możejko-Ciesielska, J., Kiewisz, R., 2016. Bacterial polyhydroxyalkanoates: Still fabulous? Microbiological Research 192, 271–282. https://doi.org/10.1016/j.micres.2016.07.010

Mukai, K., Yamada, K., Doi, Y., 1993. Enzymatic degradation of poly(hydroxyalkanoates) by a marine bacterium. Polymer Degradation and Stability 41, 85–91. https://doi.org/10.1016/0141-3910(93)90066-R

Napper, I.E., Thompson, R.C., 2020. Plastic Debris in the Marine Environment: History and Future Challenges. Global Challenges 4, 1900081. https://doi.org/10.1002/gch2.201900081

Numata, K., Abe, H., Doi, Y., 2008. Enzymatic processes for biodegradation of poly(hydroxyalkanoate)s crystals. Canadian Journal of Chemistry 86, 471–483. https://doi.org/10.1139/V08-004

Numata, K., Abe, H., Iwata, T., 2009. Biodegradability of Poly(hydroxyalkanoate) Materials. Materials 2, 1104–1126. https://doi.org/10.3390/ma2031104

Nygaard, D., Yashchuk, O., Hermida, É.B., 2021. PHA granule formation and degradation by Cupriavidus necator under different nutritional conditions. Journal of Basic Microbiology 61, 825–834. https://doi.org/10.1002/jobm.202100184

Odobel, C., Dussud, C., Philip, L., Derippe, G., Lauters, M., Eyheraguibel, B., Burgaud, G., Ter Halle, A., Meistertzheim, A.-L., Bruzaud, S., Barbe, V., Ghiglione, J.-F., 2021. Bacterial Abundance, Diversity and Activity During Long-Term Colonization of Non-biodegradable and Biodegradable Plastics in Seawater. Frontiers in Microbiology 12. https://doi.org/10.3389/fmicb.2021.734782

Oksanen, J., Kindt, R., Legendre, P., O'Hara, B., Stevens, M.H.H., Oksanen, M.J., Suggests, M., 2007. The vegan package. Community ecology package 10, 719.

Pachekoski, W.M., Agnelli, J.A.M., Belem, L.P., 2009. Thermal, mechanical and morphological properties of poly (hydroxybutyrate) and polypropylene blends after processing. Materials Research 12, 159–164. https://doi.org/10.1590/S1516-14392009000200008

Pachekoski, W.M., Dalmolin, C., Agnelli, J.A.M., 2013. The influence of the industrial processing on the degradation of poly(hidroxybutyrate) - PHB. Mat. Res. 16, 237–332. https://doi.org/10.1590/S1516-14392012005000180

Parada, A.E., Needham, D.M., Fuhrman, J.A., 2016. Every base matters: assessing small subunit rRNA primers for marine microbiomes with mock communities, time series and global field samples. Environmental Microbiology 18, 1403–1414. https://doi.org/10.1111/1462-2920.13023

Paul-Pont, I., Ghiglione, J.-F., Gastaldi, E., Ter Halle, A., Huvet, A., Bruzaud, S., Lagarde, F., Galgani, F., Duflos, G., George, M., Fabre, P., 2023. Discussion about suitable applications for biodegradable plastics regarding their sources, uses and end of life. Waste Management 157, 242–248. https://doi.org/10.1016/j.wasman.2022.12.022

Pérez-Rivero, C., Hernandez-Raquet, G., 2017. Polyhydroxyalcanoates : une alternative 'bio' aux plastiques traditionnels. Innovations Agronomiques 58, 99–112.

Prieto, A., Escapa, I.F., Martínez, V., Dinjaski, N., Herencias, C., de la Peña, F., Tarazona, N., Revelles, O., 2016. A holistic view of polyhydroxyalkanoate metabolism in Pseudomonas putida. Environ. Microbiol. 18, 341–357. https://doi.org/10.1111/1462-2920.12760

Pulido-Villena, E., Ghiglione, J.-F., Ortega-Retuerta, E., VAN-WAMBEKE, F., Zohary, T., 2012. Heterotrophic Bacteria in the Pelagic Realm of the Mediterranean Sea. Life in the Mediterranean Sea: A Look at Habitat Changes.

Quast, C., Pruesse, E., Yilmaz, P., Gerken, J., Schweer, T., Yarza, P., Peplies, J., Glöckner, F.O., 2013. The SILVA ribosomal RNA gene database project: improved data processing and web-based tools. Nucleic Acids Res 41, D590-596. https://doi.org/10.1093/nar/gks1219

Riis, V., Mai, W., 1988. Gas chromatographic determination of poly-β-hydroxybutyric acid in microbial biomass after hydrochloric acid propanolysis. Journal of Chromatography A 445, 285–289. https://doi.org/10.1016/S0021-9673(01)84535-0

Schirmer, A., Jendrossek, D., 1994. Molecular characterization of the extracellular poly(3-hydroxyoctanoic acid) [P(3HO)] depolymerase gene of Pseudomonas fluorescens GK13 and of its gene product. J Bacteriol 176, 7065–7073.

Schirmer, A., Jendrossek, D., Schlegel, H.G., 1993. Degradation of poly(3-hydroxyoctanoic acid) [P(3HO)] by bacteria: purification and properties of a P(3HO) depolymerase from Pseudomonas fluorescens GK13. Appl. Environ. Microbiol. 59, 1220–1227.

Shen, M., Huang, W., Chen, M., Song, B., Zeng, G., Zhang, Y., 2020. (Micro)plastic crisis: Un-ignorable contribution to global greenhouse gas emissions and climate change. Journal of Cleaner Production 254, 120138. https://doi.org/10.1016/j.jclepro.2020.120138

Simon, M., Azam, F., 1989. Protein content and protein synthesis rates of planktonic marine bacteria. Mar. Ecol. Prog. Ser. 51, 201–213. https://doi.org/10.3354/meps051201

Sun, Z., Ramsay, J.A., Guay, M., Ramsay, B.A., 2006. Automated feeding strategies for high-cell-density fed-batch cultivation of Pseudomonas putida KT2440. Appl Microbiol Biotechnol 71, 423–431. https://doi.org/10.1007/s00253-005-0191-7

Suzuki, M., Tachibana, Y., Kasuya, K., 2021. Biodegradability of poly(3-hydroxyalkanoate) and poly(ε-caprolactone) via biological carbon cycles in marine environments. Polym J 53, 47–66. https://doi.org/10.1038/s41428-020-00396-5

Thomas, T., Elain, A., Bazire, A., Bruzaud, S., 2019. Complete genome sequence of the halophilic PHA-producing bacterium Halomonas sp. SF2003: insights into its biotechnological potential. World J Microbiol Biotechnol 35, 50. https://doi.org/10.1007/s11274-019-2627-8

Van Wambeke, F., Ghiglione, J.-F., Nedoma, J., Mével, G., Raimbault, P., 2009. Bottom up effects on bacterioplankton growth and composition during summer-autumn transition in the open NW Mediterranean Sea. Biogeosciences 6, 705–720. https://doi.org/10.5194/bg-6-705-2009

Viljakainen, V.R., Hug, L.A., 2021. The phylogenetic and global distribution of bacterial polyhydroxyalkanoate bioplastic-degrading genes. Environmental Microbiology 23, 1717–1731. https://doi.org/10.1111/1462-2920.15409

Volant, C., Balnois, E., Vignaud, G., Magueresse, A., Bruzaud, S., 2022. Design of Polyhydroxyalkanoate (PHA) Microbeads with Tunable Functional Properties and High Biodegradability in Seawater. J Polym Environ 30, 2254–2269. https://doi.org/10.1007/s10924-021-02345-6

Volova, T.G., Boyandin, A.N., Vasil'ev, A.D., Karpov, V.A., Kozhevnikov, I.V., Prudnikova, S.V., Rudnev, V.P., Xuản, B.B., Dũng, V.V., Gitel'zon, I.I., 2011. Biodegradation of polyhydroxyalkanoates (PHAs) in the South China Sea and identification of PHA-degrading bacteria. Microbiology 80, 252–260. https://doi.org/10.1134/S0026261711020184

Wickham, H., 2016. ggplot2: elegant graphics for data analysis. Springer-Verlag New York, 2016. Springer-Verlag New York.

Wright, R.J., Erni-Cassola, G., Zadjelovic, V., Latva, M., Christie-Oleza, J.A., 2020. Marine Plastic Debris: A New Surface for Microbial Colonization. Environ Sci Technol 54, 11657–11672. https://doi.org/10.1021/acs.est.0c02305

Xie, Y., Noda, I., Akpalu, Y.A., 2008. Influence of cooling rate on the thermal behavior and solid-state morphologies of polyhydroxyalkanoates. Journal of Applied Polymer Science 109, 2259–2268. https://doi.org/10.1002/app.28278

Young, K.D., Chul, K.H., Young, K.S., Ha, R.Y., 2005. Molecular Characterization of Extracellular Medium-chain-length Poly(3-hydroxyalkanoate) Depolymerase Genes from Pseudomonas alcaligenes Strains. Journal of Microbiology 43, 285–294.

Zettler, E.R., Mincer, T.J., Amaral-Zettler, L.A., 2013. Life in the “Plastisphere”: Microbial Communities on Plastic Marine Debris. Environ. Sci. Technol. 47, 7137–7146. https://doi.org/10.1021/es401288x

Appendices

Appendix A: DSC curves of the 6 PHA solvent-casted films

PHB

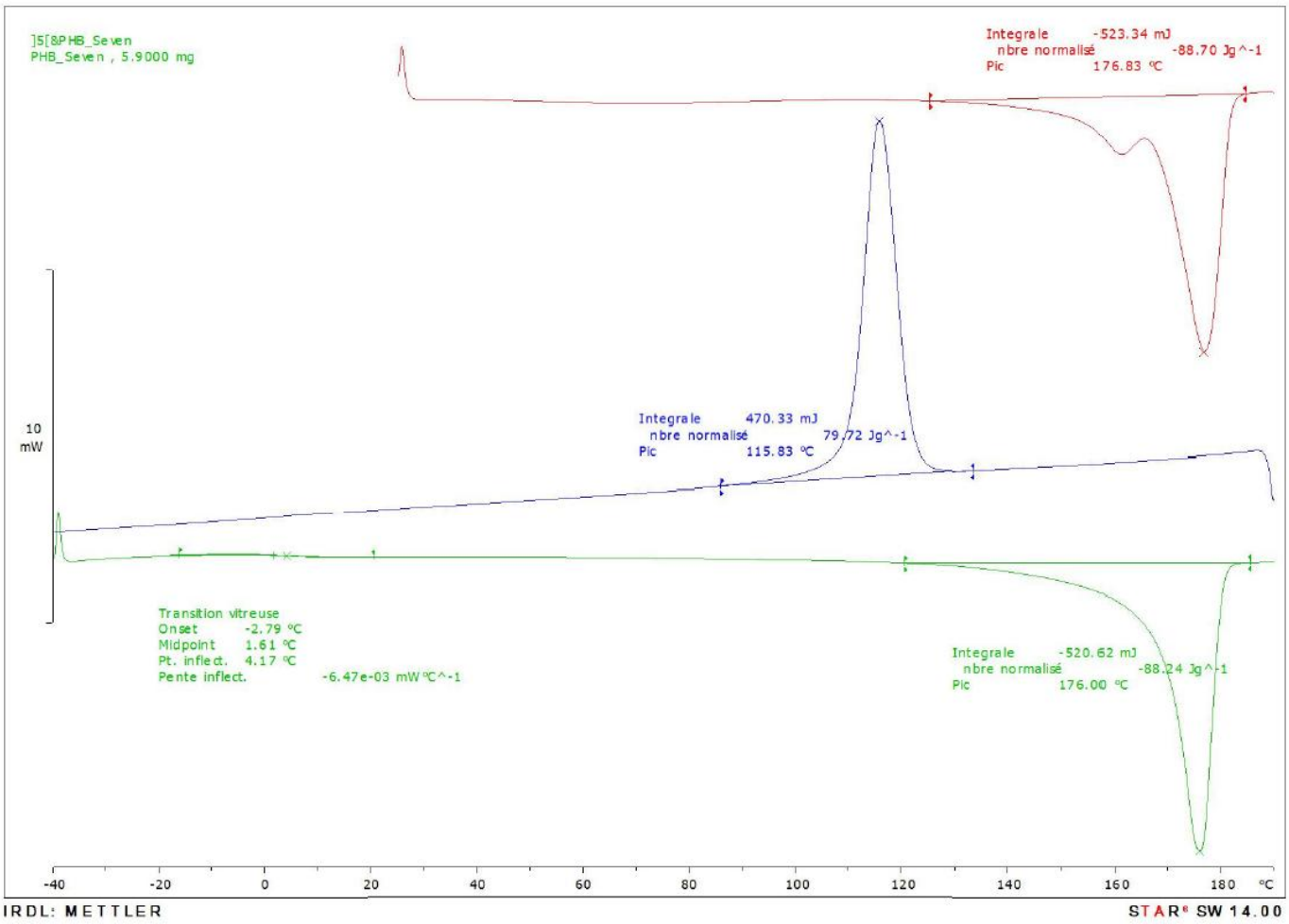

PHBHV6

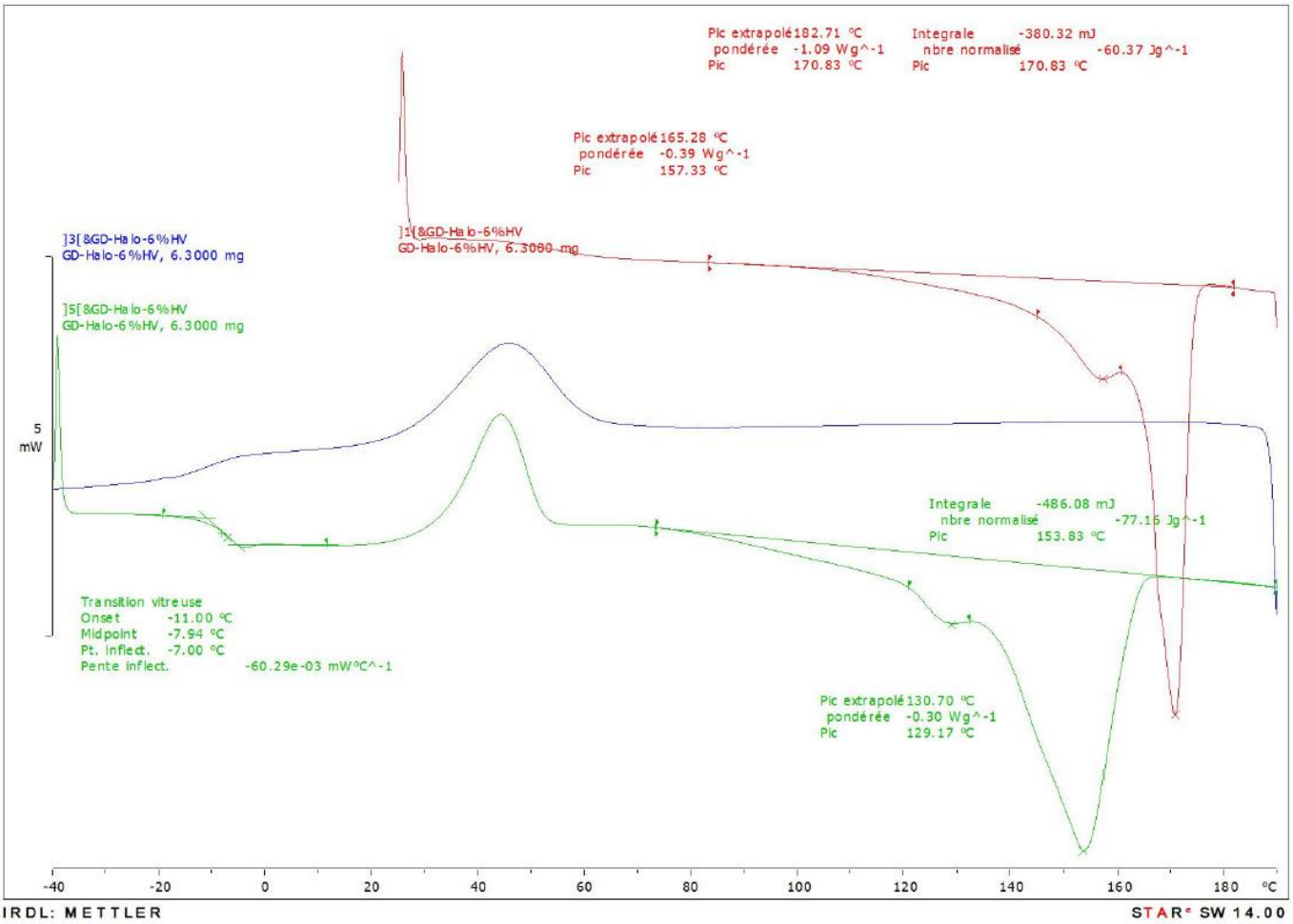
Pic extrapolé 182.71 °C
pondérée -1.09 Wg^-1
Pic 170.83 °C
Integrale -380.32 mJ
nbre normalisé -60.37 Jg^-1
Pic 170.83 °C
Pic extrapolé 165.28 °C
pondérée -0.39 Wg^-1
Pic 157.33 °C
]1[&GD-Halo-6%HV
GD-Halo-6%HV, 6.3000 mg
]3[&GD-Halo-6%HV
GD-Halo-6%HV, 6.3000 mg
]5[&GD-Halo-6%HV
GD-Halo-6%HV, 6.3000 mg
5
mW
Integrale -486.08 mJ
nbre normalisé -77.16 Jg^-1
Pic 153.83 °C
Transition vitreuse
Onset -11.00 °C
Midpoint -7.94 °C
Pt. inflect. -7.00 °C
Pente inflect. -60.29e-03 mW°C^-1
Pic extrapolé 130.70 °C
pondérée -0.30 Wg^-1
Pic 129.17 °C
-40
-20
0
20
40
60
80
100
120
140
160
180
°C
IRDL: METTLER
STAR° SW 14.00

PHBHV11

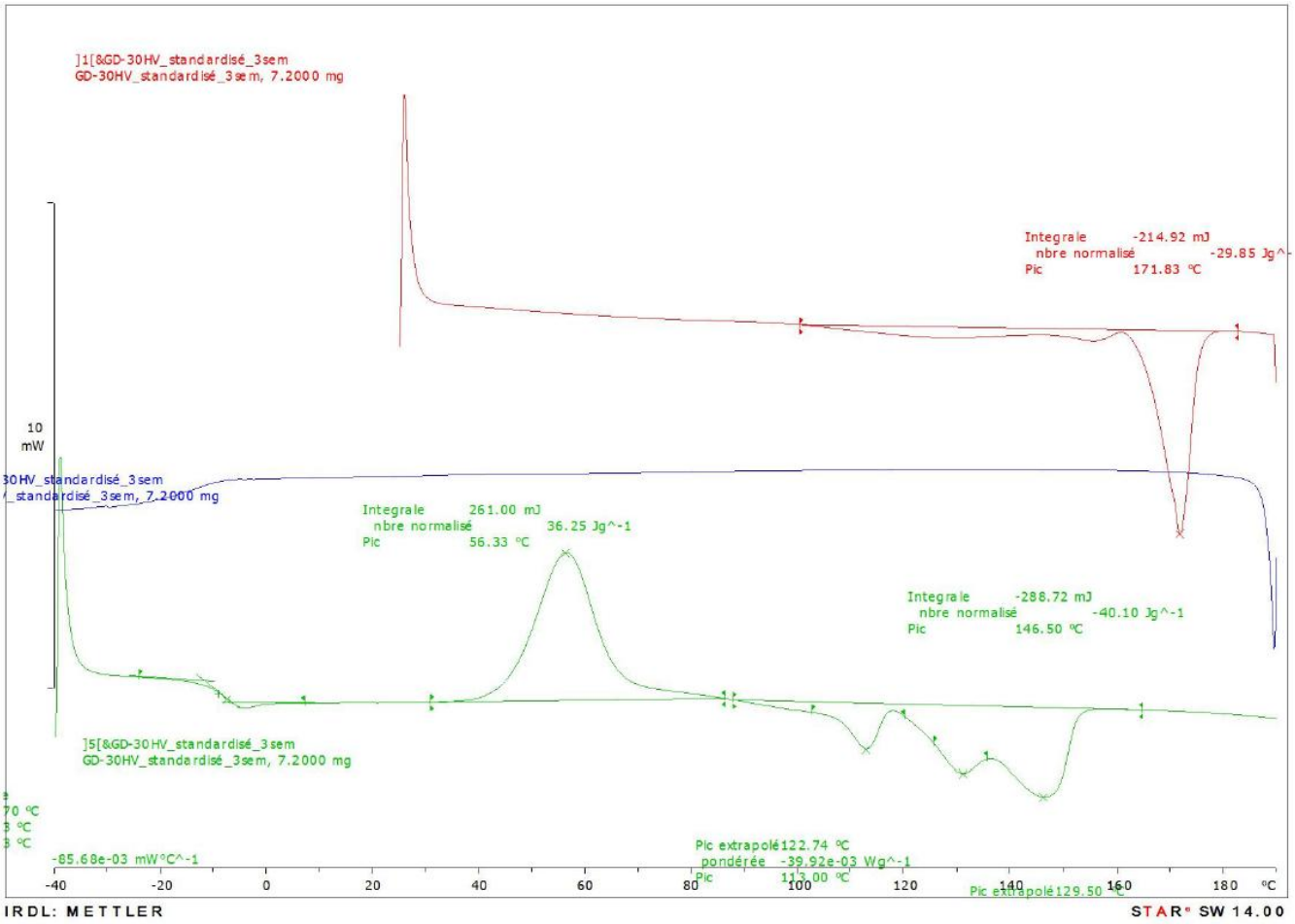
]1[&GD-30HV_standardisé_3sem
GD-30HV_standardisé_3sem, 7.2000 mg
Integrale -214.92 mJ
nbre normalisé -29.85 Jg^-
Pic 171.83 °C
10
mW
30HV_standardisé_3sem
_standardisé_3sem, 7.2000 mg
Integrale 261.00 mJ
nbre normalisé 36.25 Jg^-1
Pic 56.33 °C
Integrale -288.72 mJ
nbre normalisé -40.10 Jg^-1
Pic 146.50 °C
]5[&GD-30HV_standardisé_3sem
GD-30HV_standardisé_3sem, 7.2000 mg
70 °C
3 °C
3 °C
-85.68e-03 mW°C^-1
Pic extrapolé122.74 °C
pondérée -39.92e-03 Wg^-1
Pic 113.00 °C
Pic extrapolé129.50 °C
-40
-20
0
20
40
60
80
100
120
140
160
180
°C
IRDL: METTLER
STAR° SW 14.00

PHO

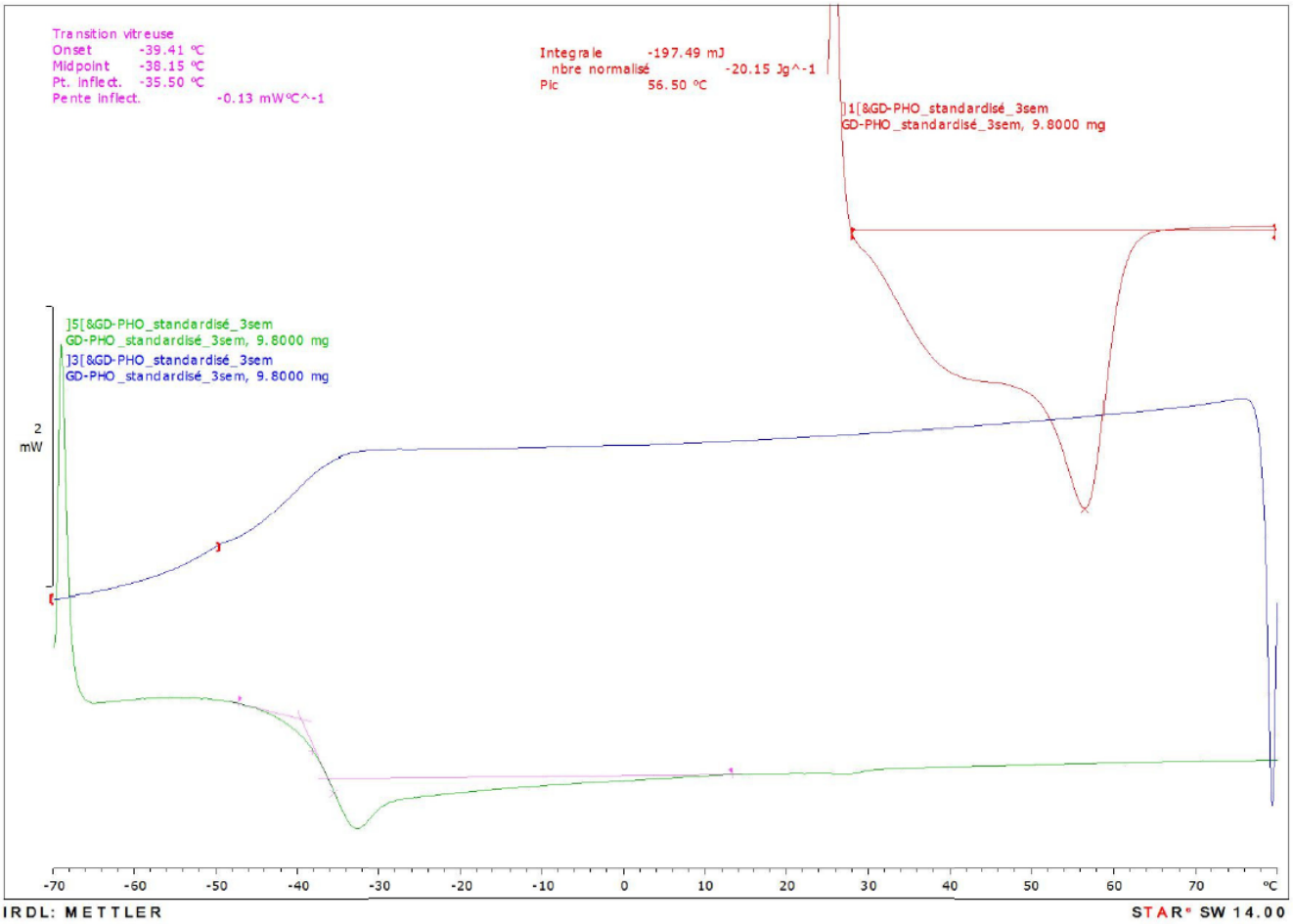
Transition vitreuse
Onset -39.41 °C
Midpoint -38.15 °C
Pt. inflect. -35.50 °C
Pente inflect. -0.13 mW°C^-1
Integrale -197.49 mJ
nbre normalisé -20.15 Jg^-1
Pic 56.50 °C
]1[&GD-PHO_standardisé_3sem
GD-PHO_standardisé_3sem, 9.8000 mg
]5[&GD-PHO_standardisé_3sem
GD-PHO_standardisé_3sem, 9.8000 mg
]3[&GD-PHO_standardisé_3sem
GD-PHO_standardisé_3sem, 9.8000 mg
2
mW
-70
-60
-50
-40
-30
-20
-10
0
10
20
30
40
50
60
70
°C
IRDL: METTLER
STAR® SW 14.00

PHN

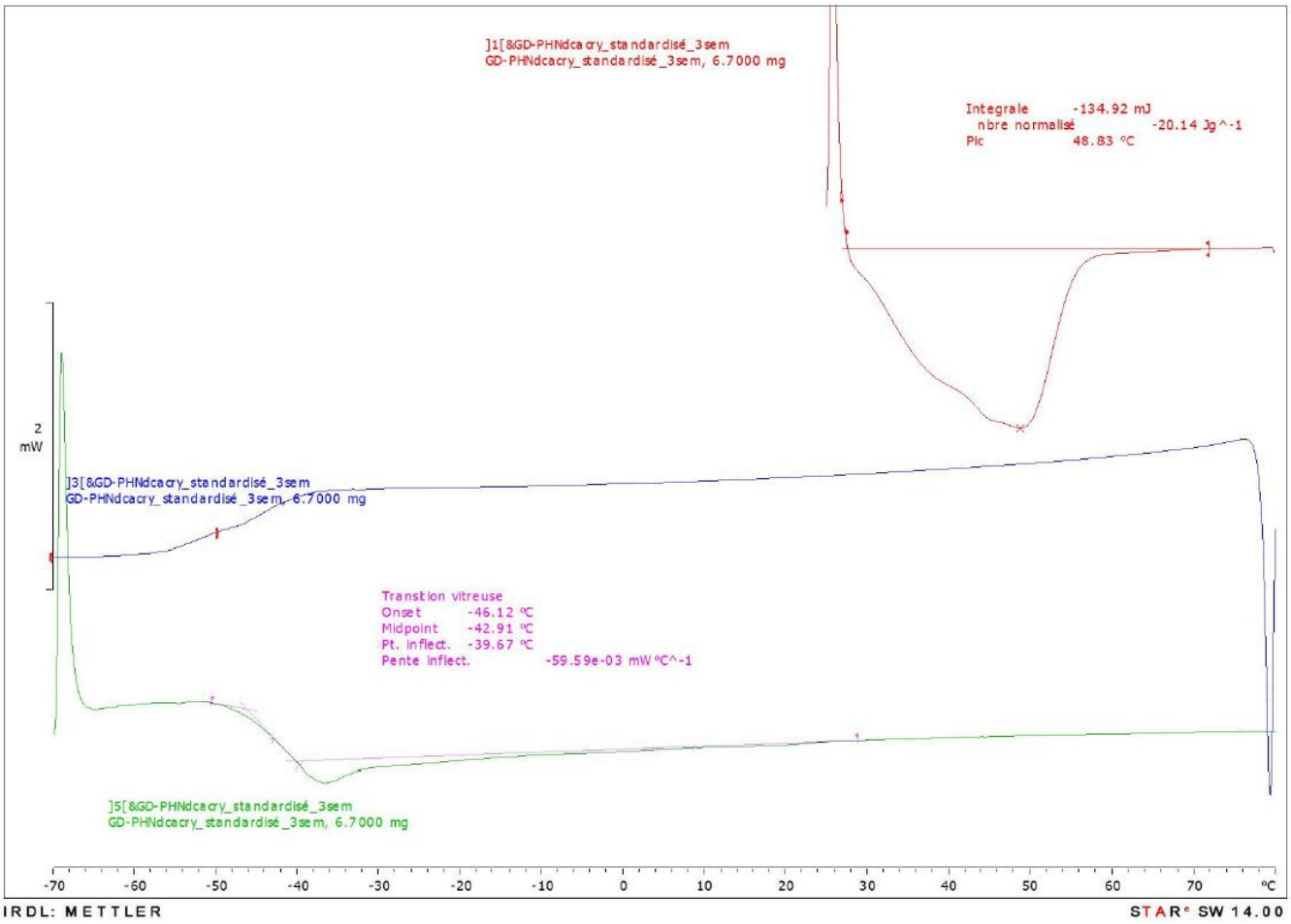
]1[&GD-PHNdcacry_standardisé_3sem
GD-PHNdcacry_standardisé_3sem, 6.7000 mg
Integrale -134.92 mJ
nbre normalisé -20.14 Jg^-1
Pic 48.83 °C
2
mW
]3[&GD-PHNdcacry_standardisé_3sem
GD-PHNdcacry_standardisé_3sem, 6.7000 mg
Transition vitreuse
Onset -46.12 °C
Midpoint -42.91 °C
Pt. inflect. -39.67 °C
Pente inflect. -59.59e-03 mW °C^-1
]5[&GD-PHNdcacry_standardisé_3sem
GD-PHNdcacry_standardisé_3sem, 6.7000 mg
-70 -60 -50 -40 -30 -20 -10 0 10 20 30 40 50 60 70 °C
IRDL: METTLER
STAR SW 14.00

PHNac

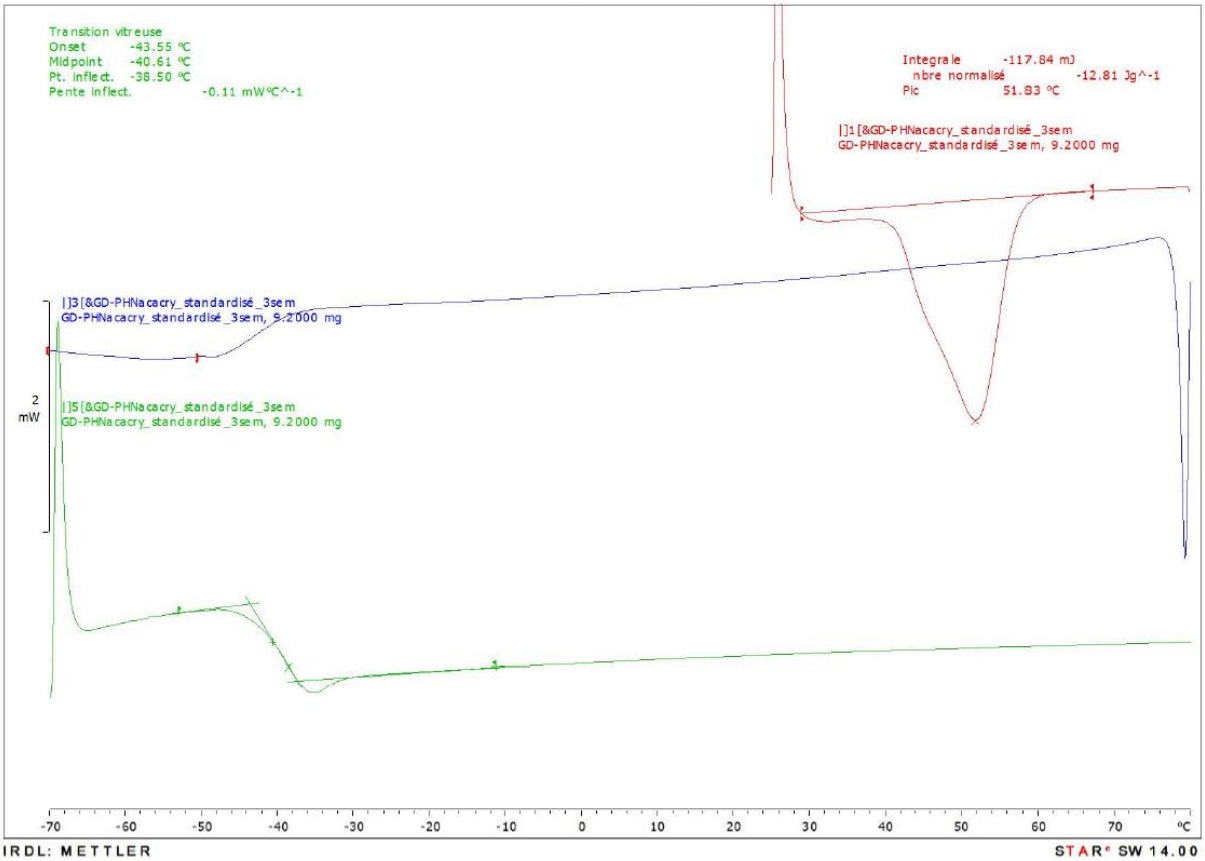
Transition vitreuse
Onset -43.55 °C
Midpoint -40.61 °C
Pt. inflect. -38.50 °C
Pente inflect. -0.11 mW°C^-1
Integrale -117.84 mJ
nbre normalisé -12.81 Jg^-1
Pic 51.83 °C
|]1[&GD-PHNacacry_standardisé_3sem
GD-PHNacacry_standardisé_3sem, 9.2000 mg
|]3[&GD-PHNacacry_standardisé_3sem
GD-PHNacacry_standardisé_3sem, 9.2000 mg
|]5[&GD-PHNacacry_standardisé_3sem
GD-PHNacacry_standardisé_3sem, 9.2000 mg
2
mW
-70 -60 -50 -40 -30 -20 -10 0 10 20 30 40 50 60 70 °C
IRDL: METTLER
STAR® SW 14.00

Appendicx B:

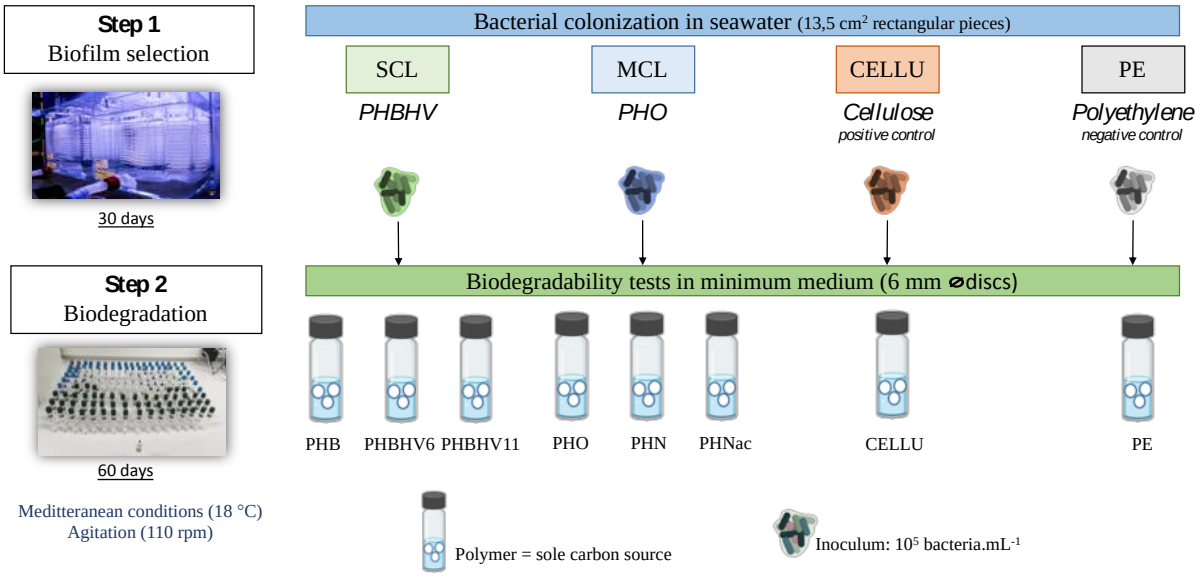

Appendix C:

Minimal medium composition : : NaCl 24 $g.L^{-1}$, Na_2SO_4 4 $g.L^{-1}$, KCl 0.68 $g.L^{-1}$, KBr 0.1 $g.L^{-1}$, H_3BO_3 0.025 $g.L^{-1}$, NaF 0.002 $g.L^{-1}$, $MgCl_2{\cdot}6H_2O$ 10.8 $g.L^{-1}$, $CaCl_2{\cdot}2H_2O$ 1.5 $g.L^{-1}$, $SrCl_2{\cdot}6H_2O$ 0.024 $g.L^{-1}$, $NaHCO_3$ 0.2 $g.L^{-1}$, $NaHPO_4$ 0.04 $g.L^{-1}$, NH_4Cl 0.5 $g.L^{-1}$, $FeCl_3$ 4 $g.L^{-1}$, EDTA 2 $g.L^{-1}$, 1 mL of traces elements for 1 L of medium composed of: $CuCl_2{\cdot}2H_2O$ 0.015 $g.L^{-1}$, $NiCl_2{\cdot}H_2O$ 0.025 $g.L^{-1}$, $Na_2MoO_4{\cdot}2H_2O$ 0.025 $g.L^{-1}$, $ZnCl_2$ 0.07 $g.L^{-1}$, $MnCl_2{\cdot}4H_2O$ 0.1 $g.L^{-1}$, $Cocl_2{\cdot}6H_2O$ 0.12 $g.L^{-1}$ and 1 mL of a vitamin solution for 1 L of medium composed of: p-aminobenzoic acid 0.005 $g.L^{-1}$, pyridoxine-HCl 0.1 $g.L^{-1}$, thiamine-HCl 0.05 $g.L^{-1}$, riboflavin 0.05 $g.L^{-1}$, nicotinic acide 0.05 $g.L^{-1}$, D-Ca-pantothenate 5.10^{-9} $g.L^{-1}$, lipoic acid 0.05 $g.L^{-1}$, nicotinamide 0.05 $g.L^{-1}$, B12 vitamin 0.05 $g.L^{-1}$, biotine 0.02 $g.L^{-1}$ and folic acid 0.02 $g.L^{-}1$.

Appendix D : Evolution of the number average molecular weight ($g.mol^{-1}$) at Day 0, Day 60 and of abiotic control (PHA but no bacteria) at Day 60.

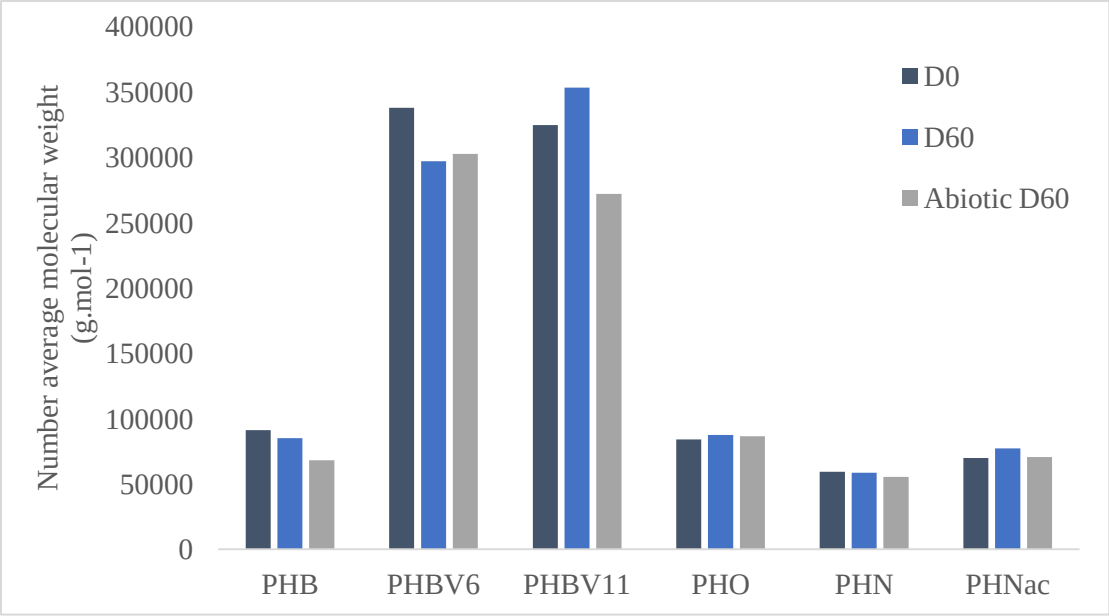
Number average molecular weight (g.mol-1)
400000
350000
300000
250000
200000
150000
100000
50000
0
PHB
PHBV6
PHBV11
PHO
PHN
PHNac
D0
D60
Abiotic D60